Magmatic Processes: Physicochemical Principles
© The Geochemical Society, Special Publication No. 1, 1987
Editor B. O. Mysen

Neutral buoyancy and the mechanical evolution of magmatic systems

MICHAEL P. RYAN
Branch of Igneous and Geothermal Processes, 959 National Center,
U.S. Geological Survey, Reston, Virginia 22092 U.S.A.

What once sprung from
the Earth sinks back
into the Earth.

Lucretius (99–55 B.C.)

Abstract—Regions of neutral buoyancy are produced by the crossover in the *in-situ* densities of magmatic fluids and the countryrock of subcaldera magma reservoirs and rift systems. Beneath this horizon, magmatic parcels ascend under positive buoyancy forces, where above it, they descend under the influence of negative buoyancy. In Hawaii, the region of neutral buoyancy is coincident with the location of the summit reservoirs of Kilauea and Mauna Loa volcanoes. The horizon of neutral buoyancy, coupled with the contractancy mechanism which produces it, thus provides for the long-term stability (the prolonged existence) of subcaldera magma reservoirs, and their rift systems. As Hawaiian volcanoes evolve, they carry their contractancy profile and region of neutral buoyancy upward with them. Thus the evolutionary progression from seamount, through a subaerial immature shield, to a mature volcano, is one characterized by the progressive elevation of the summit reservoir complex and rift zones—a process that leaves beneath a wake of high velocity mafic and ultramafic rocks within the core region of the shield. In Iceland, the upper levels of the depth range for subcaldera magma storage and lateral injection in the active rift zones of the Krafla central volcano are coincident with the horizon of neutral buoyancy. Intrusion dynamics at Krafla, analogous to that of Kilauea's rift zones, demonstrate that the depth interval 2 to 4 km contains the parabolic nose of the expanding magmatic fracture front—symmetrically moving along the horizon of neutral buoyancy. Along the East Pacific Rise at 21°N latitude, and near the Siqueiros Fracture Zone, regions of marked reduction in elastic wave velocity at depth intervals of 2.5–4.5 km and 2.0–3.5 km, respectively, are inferred to contain partial melt and are consistent with the location of a horizon of neutral buoyancy. This suggests that neutral buoyancy, and the related changes in *in-situ* density produced through crustal contractancy, play a fundamental role in the inception, dynamics and evolution of magma reservoirs and their intrusive complexes within the Earth's oceanic spreading centers. Moreover, inspection of the magma and countryrock densities relevant to regions of calc-alkaline volcanism above subduction zones, and at select centers of granitic–rhyolitic complexes in continental interiors, suggest that their upper levels have a depth extent regulated by the neutral buoyancy principle.

INTRODUCTION

MAGMATIC FLUIDS, generated at depth in the Earth's mantle often come to rest at surprisingly shallow levels within the crust. It is, of course, remarkable that so long an odyssey should be interrupted just short of subaerial or submarine eruption. But such interruptions in the form of shallow crustal intrusive events are widespread, long-lived, and have played an enduring and important role in the evolution of the Earth's crust.

Why does magma come to rest at shallow levels in the crust? That is, why do shallow magma reservoirs exist? What are the mechanical controls that regulate the growth and evolution of subcaldera magma reservoirs and their associated rift systems? How do these controls operate within the context of the short-term dynamics of a volcanic system and its longer term evolutionary trends? Are there important mechanical and dynamic processes whose controls are, in part, independent of the deeper geodynamic regimes that support and feed them? In this paper, these questions will be addressed by presenting a series of relations that exist between the space-time behavior of shallow magmatic storage and transport regimes, pressure-dependent physical properties of the mafic and ultramafic rocks that surround them, and the magma contained within.

As active Hawaiian volcanoes grow upward, their summit magma reservoirs rise progressively. Such a pattern was suggested by JACKSON (1968) and HILL (1969) to explain the roughly cylindrical core of ultramafic cumulates inferred on the basis of high compressional wave velocities within active and extinct Hawaiian volcanoes. Gravity surveys (KINOSHITA, 1965; KINOSHITA and OKAMURA, 1965; Hawaii Institute of Geophysics, 1965) have demonstrated that this pattern of high density volcanic cores exists throughout the Hawaiian archipelago,

and must, therefore, represent a fundamental process in the construction of Hawaiian shields. Recently, DECKER *et al.* (1983) have geodetically confirmed this trend of upward reservoir growth, by demonstrating that the relative position of Mauna Loa's (elevation: 4,169 meters above mean sea level (AMSL)) summit reservoir is approximately the same as its diminutive younger neighbor, Kilauea (elevation: 1,240 meters AMSL) (Figure 1). That is, for each volcano, the magma reservoir roof lies at $\approx$2 km depth, and the depth inferred for the central region of pressure lies near 3 km respectively, beneath their summit calderas. The reasons for this relationship were not, however, suggested by these authors (DECKER *et al.*, 1983), and although confirmed, it has remained puzzling why such a systematic pattern should occur.

Since the recognition that Icelandic crustal accretion is intimately bound up in the plate margin accretionary process itself (BODVARSSON and WALKER, 1964; PÁLMASON and SAEMUNDSSON, 1974) it has been determined—partly through the study of the dissected Tertiary volcanoes in the eastern fjörds (WALKER, 1959, 1963)—that the emplacement of intrusives progressively stretches the Icelandic crust. Confirmation of this crustal stretching, and its role in the plate accretion process, has been documented through geodetic studies of the current magmatic episode at the Krafla central volcano (BJÖRNSSON *et al.* 1979; TRYGGVASON 1980, 1984, 1986). Similarly, whereas the geodetic signature of crustal evolution and plate accretion has been firmly established, the mechanical controls have not been made clear.

DEFINITIONS

Contractancy may be defined as the progressive reduction in macroscopic and microscopic pore space as a function of increases in depth and confining pressure. A central element in the definition is the progressive sealing shut—or contraction—of fractures, joints and irregular inter-flow porosity with depth. A synthesis of the structural geology of active rift systems and their *in-situ* compressional wave velocity structure from seismic refraction experiments, suggests that the large-scale vertical fractures form an important component of closable shallow porosity. It may be thought of as an anelastic volume decrease under applied loading, and is distinguished from dilantancy—the anelastic increase in volume under differential stresses. The importance of the mechanism of contractancy lies in its ability to change significantly the *in-situ* density of the uppermost fractured veneer of rock above active magma reservoirs and rift systems, and in so doing, produces horizons of neutral buoyancy and magma stabilization. Within a geotechnical and engineering mechanics context, the term has an established usage fully consistent with the physical mechanism under discussion here: the progressive closure of dilatant cracks under increasing normal stress components. For example, GOODMAN and DUBOIS (1972) and GOODMAN (1976) discuss the closure history of cracks as functions of normal and shear stress components, present constitutive relations for jointed media, and outline the relative roles of contractancy and dilatancy in fractured media deformation. The term contractancy thus has an established usage, a succinctness that obviates the need for a more lengthy description, and the ability to clearly convey a physical mechanism.

Neutral buoyancy is produced by an equity in the effective, large-scale *in-situ* density of magma and the host countryrock. As such, the net driving force for vertical motion has been removed, and the magmatic structure or region has been stabilized. No restrictions are placed on the geologic context within which neutral buoyancy can be achieved; that is, within magma chambers, multiply-connected magma reservoirs, dikes, sills or structures of other geometries. Implicit in the definition is the concept of an integrated or net equity between the fluid components of an active magma reservoir and the far–field host countryrock. It is emphasized that the concept focuses on the long–term stability of a magmatic region or major structural subdivision of a magmatic system. In addition, it provides a control on the geometry, location and dynamics of dike emplacement that are laterally-directed from high-level reservoirs.

The horizon of neutral buoyancy is that depth interval within which the magma density and the aggregate country rock density are equal. It is expected to have a narrow vertical extent, and wide lateral extent. In three dimensions, it is not a plane, but rather a layer having its own topography, as produced by local heterogenieties in country rock composition and local variations in porosity and structure. The wide lateral extent of the horizon of neutral buoyancy is a primary control on the depth of magma injection: it corresponds to the locus of the parabolic magma fracture front during the dike formation process. It's lateral extent corresponds, therefore, to the maximum lateral reach of magmatic injection within an active rift zone. In this fashion, local and regional horizons of neutral buoyancy may be integrated, to form surfaces of neutral buoyancy with regional, plate or global dimensions. It may be contrasted with the region of neutral buoyancy, which, as used in this paper, has a finite depth extent and a lateral extent that is restricted to the dimensions of subcaldera magma storage.

THE PHENOMENOLOGY OF ROCK CONTRACTANCY

A characteristic feature of the pressure dependence of compressional wave velocities in the mafic and ultramafic rocks of Hawaii and Iceland, is the nonlinear increase in V_p with increasing confining pressure. Figures 2, 3, and 4 illustrate this behavior to 1000 MPa. In general, V_p and its pressure dependence, $\partial V_p/\partial P$, show two types of behavior: a low pressure, non-linear dependence, ranging from 0 to 200 MPa, and a second, generally linear regime that starts at 200 MPa, and extends to higher pressures. Since the work of BIRCH (1960), studies of dry holocrystalline rocks (TODD and SIMMONS, 1972), as well as fluid-saturated porous lithologies (KING, 1966), have attributed this change in wave velocity to the progressive closure of microfractures within the rock matrix. This microfracture closure—or contractancy—produces the early rapid rise in V_p and V_s characteristic of the low pressure environment.

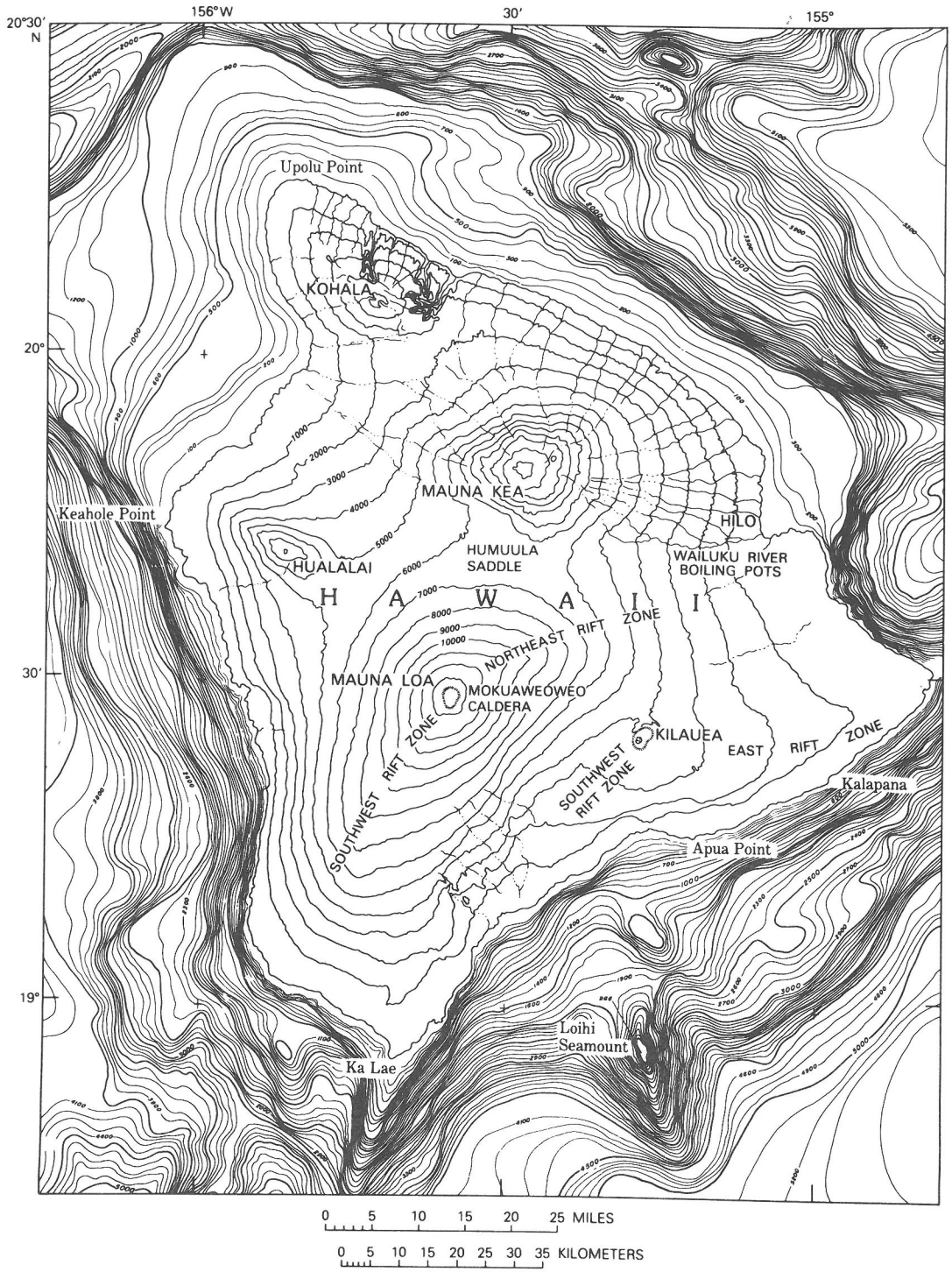

FIG. 1. The island of Hawaii, and three centers of active volcanism in progressive stages of their life cycle: Loihi Seamount, Kilauea and Mauna Loa. The evolutionary progression of their subcaldera magma reservoirs is illustrated in vertical cross-section in Figure 11. Marine bathymetry is based on the compilation of CHASE *et al.* (1980), and contours are in meters. Topographic contours above mean sea level are in feet.

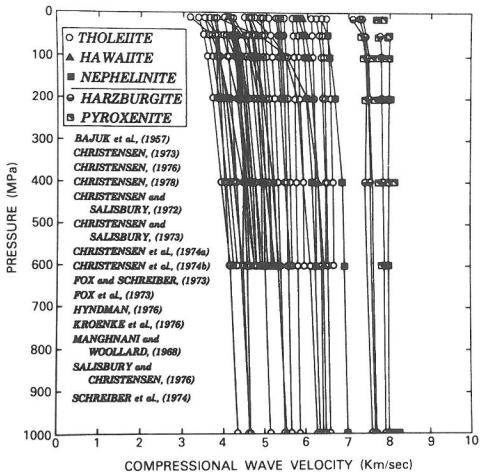

FIG. 2. The pressure dependence of compressional wave velocities (V_p) in the tholeiitic, alkalic and nephelinitic basalt of Hawaiian shield volcanoes, and in the rocks of their ultramafic upper mantle foundations. Particularly noteworthy is the non-linear behavior of V_p at confining pressures below 200 MPa.

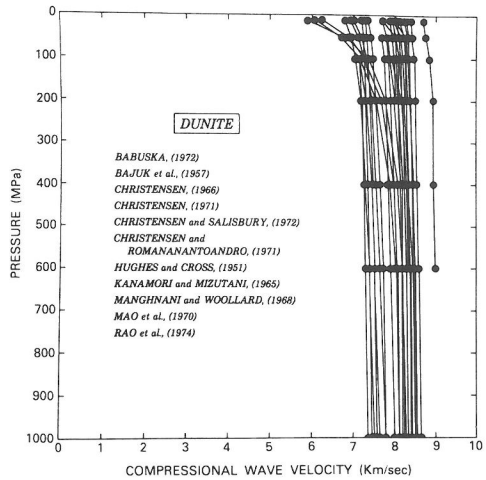

FIG. 4. The pressure dependence of compressional wave velocity (V_p) in dunite. For olivine-rich cumulates that may floor shallow storage compartments in subcaldera reservoirs, or plate the walls of deep rift zone conduits, the non-linear sections of the compressional wave curves are expected to apply.

The linear change in wave velocity above 200 MPa, is produced by the compressibility of the minerals within the matrix (BIRCH, 1960). Additional evidence of the important changes in the mechanical and transport properties of crystalline igneous rocks as confining pressures change in the near-surface environment are (see Figure 5): (1) order of magnitude increases in fluid permeability over the range 200 to 0.1 MPa, (BRACE, 1972); (2) increases in compressibility over 800 to 0.1 MPa (BRACE, 1972); (3) order of magnitude increases in d.c. electrical conductivity for fluid-saturated rocks over the range 300 to 0.1 MPa; (BRACE and ORANGE, 1968a,b); and (4) corresponding decreases in aggregate thermal conductivity over the range 100 MPa to 0.1 MPa (BRACE, 1972). These confining pressure ranges have depth equivalents that extend into the magma storage regions of the active volcanoes in Hawaii, in Iceland and in the Earth's mid–ocean rift systems. Thus, these mechanical and transport properties will all exhibit the characteristic non-linear behavior induced by the low confining pressures associated with the Earth's surface, in countryrock that surrounds subcaldera and central reservoirs and their radiating rift systems. In Figure 5, those properties that characterize a mechanical response to applied loading (V_p, V_s, β, K and μ) are referred to as aggregate mechanical properties, whereas the transport of heat ($\bar{K}$) and pore fluids (K_f) are referred to as aggregate transport properties.

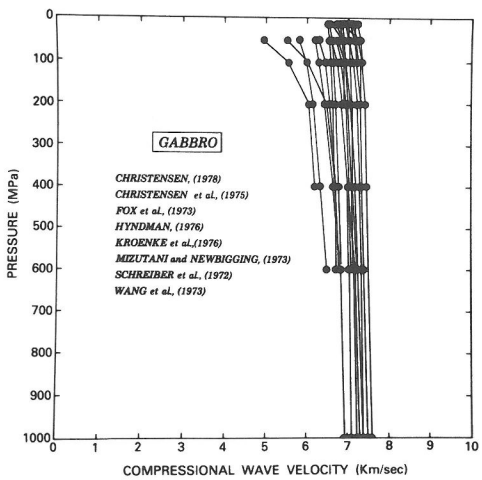

FIG. 3. The pressure dependence of compressional wave velocity in gabbro. Such a confining pressure dependence is expected to characterize the intact gabbroic masses in rift zone and central region cores. Changes in the pressure derivative of V_p ($\partial V_p/\partial P$) above and below 200 MPa, are suggestive of the progressive closure of microcracks within the upper levels of the volcanic shield.

CONTRACTANCY WITHIN VOLCANIC CENTERS

The superstructures of active Hawaiian and Icelandic volcanoes contain evidence of dilatant fractures—void spaces that are inferred to extend to depths approaching 2 km. This evidence includes the following:

(1) gaping cracks in rift systems and summit calderas, which can have crack opening displacements from 10's of centimeters to meters (*e.g.*, the "Great Crack" of Kilauea's southwest rift zone and the dilatant fracture network of the Námafjall-Krafla–Gjástykki rift system);

(2) exceptionally low compressional wave velocities within the upper two kilometers (≈2.5 km/

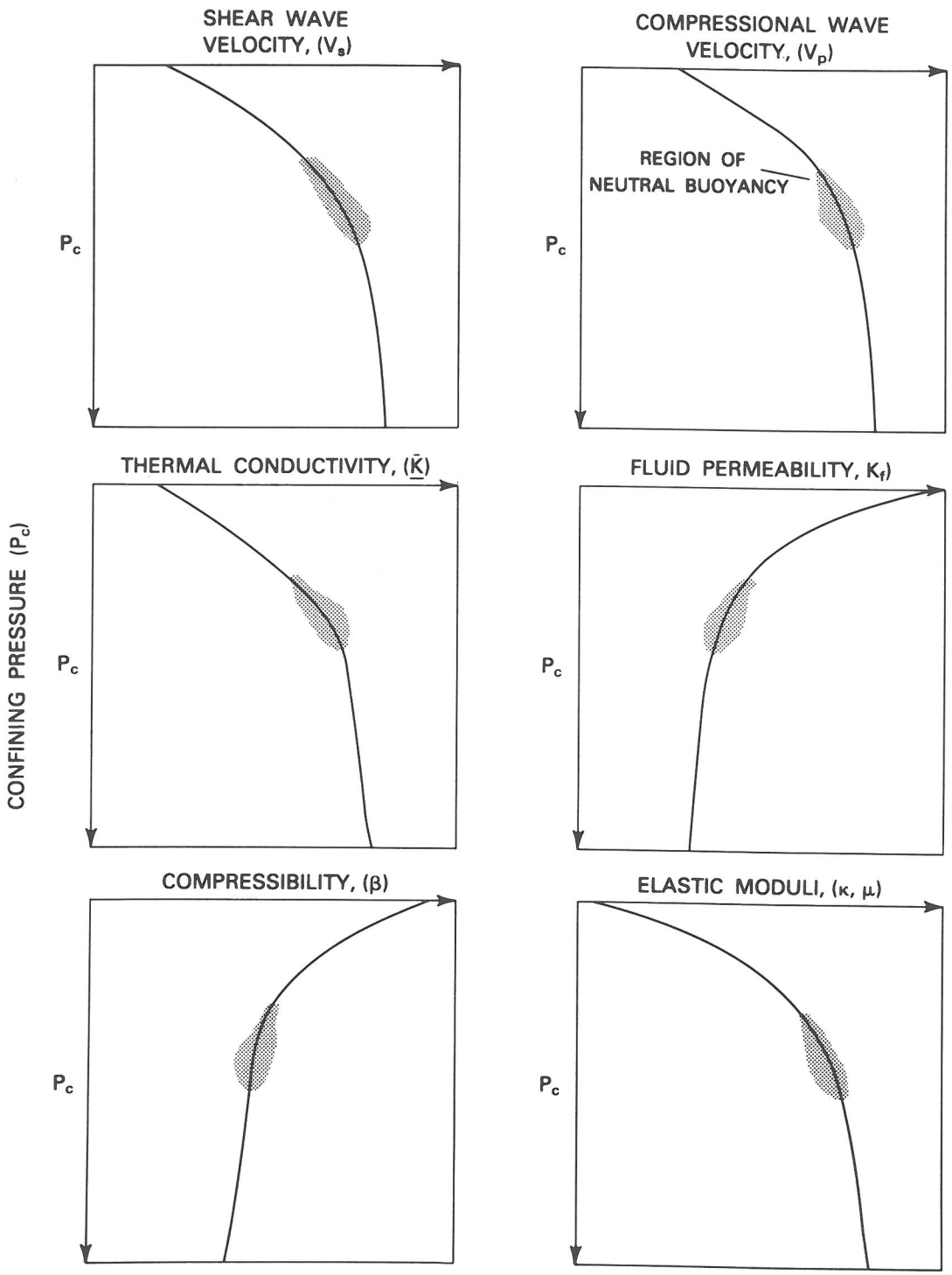

FIG. 5. The synoptic pressure dependence of the mechanical (V_s, V_p, β, K, and μ) and transport ($\bar{K}$ and K_f) properties of mafic and ultramafic rocks under the low to moderate confining pressures appropriate to shallow magma storage in oceanic shield volcanoes, central volcanoes and their associated rift zones, and in mid–ocean spreading centers. These properties have been schematically summarized, and are based on the studies of BRACE (1971a, 1972), BRACE and ORANGE (1968a,b), the combined compilations of Figures 2, 3 and 4, as well as WALSH (1965, 1981) and WALSH and DECKER (1966).

sec for Hawaii (ZUCCA *et al.*, 1982) and ≈2.0–2.5 km/sec for Iceland (FLOVENZ, 1980; FLOVENZ *et al.*, 1985).

(3) exceptionally low *in-situ* densities within the upper two kilometers; (ZUCCA *et al.*, 1982; PÁLMASON, 1963, 1971).

(4) the common observation of massive lava drainback at the conclusion of an eruptive phase, as well as the observations of concurrent eruption and drainback, as exemplified by the 1983 activity at Pu'u O'o, in Kilauea's east rift zone, and completely analogous activity in the Gjástykki rift system north of the Krafla caldera;

(5) the long-observed discrepancy between the vertical and horizontal displacement fits to geodetic model predictions, suggesting considerable horizontal inelastic behavior at shallow depths (see RYAN *et al.*, 1983, pp. 4150–4152).

The depth intervals inferred for Kilauea's summit magma reservoir have been compiled in Figure 6a. These constraints are based on (a) three–dimensional deformation modeling (RYAN *et al.*, 1983); (B) three-dimensional studies of the seismicity associated with the hydraulic inflation of the summit reservoir (RYAN *et al.*, 1981); (c) simply-connected models of the reservoir as sources of pressure or displacement (*e.g.*, MOGI, 1958); and (d) inversions of summit tilt, trilateration and displacement data (*e.g.*, DVORAK *et al.*, 1983). The total depth range is ≈2 to 9 km, including the reservoir "roots." Uncertainties in the geodetic and seismic resolution of depth intervals typically span the range 500 m to 1000 m. Because 15 of the 16 studies of these depth ranges are included within the 2 to 4 km interval, this is the most frequently retrieved interval for subcaldera magma storage. On purely geometric grounds, however, the interval 2.2 to 3.5 km, for example, also encompasses this same 15-study consensus. As such, it explicitly acknowledges the uncertainties in both the seismic and the geodetic resolution. The aseismic region beneath Kilauea caldera extends to a depth of 6 to 7 km, thus suggesting that the geodetic studies tend to 'see' the upper levels of the reservoir. The seismic surveys must therefore be taken into greater account when evaluating the total depth range available for storage.

Within the Hawaiian and Icelandic crust, we expect to find the fracture porosity saturated with water. It is relevant then to consider the contractancy of basalt with both dry and H_2O–saturated porosity and its pressure dependence. This dependence is illustrated in Figure 6b for basalt (CHRISTENSEN and SALISBURY, 1975). The characteristic $\partial V_p/\partial p$—non-linear for pressures less than 200 MPa—is well developed, especially for the "dry" curve where the fluid-accessible fracture space is occupied by air. Both the dry and H_2O–saturated curves show an additional effect: there is a pressure interval above which (in the direction of increasing pressure) the pore space accessible to the mobile second phase (air or H_2O) has been squeezed out. For basalt, gabbro, and dunite, this pressure window comprises a transition region centered at 200–300 MPa. This region of transition coincides with the convergence of the fluid-saturated and dry branches, and is herein referred to as the contractancy transition zone. The zone separates the figure into two subregions: a shallow region where the dominant mechanism is the compression of fractures and pore fluids, and a deeper region dominated by the compression of the crystal structures in the component mineral phases, as well as intercrystalline glass.

A comparison of Figures 6a and 6b makes clear the 1:1 correlation between the depth range associated with magmatic storage, and the equivalent confining pressure-depth level required for the elimination of fluid-accessible fracture porosity in basalt. This transition, from the compression of pore fluids and fracture space above 9 km, to the compression of minerals below 10 km, is illustrated by the schematic volume elements in Figure 6b, and denoted by a stippled region in both figures.

CONTRACTANCY AND SUBCALDERA MAGMA STORAGE

If the bulk compression of the volcanic system is dominated—at shallow levels—by the progressive elimination of macrofracture, joint, microfracture and vesicle porosity due to increasing confining pressure, then we should expect to see correlation between the *in-situ* density of the volcanic superstructure and increases in confining pressure. Moreover, the systematics of the mechanical and transport properties with depth, as exemplified by changes in the compressional and shear wave velocities ($\partial V_p/\partial Z$, $\partial V_s/\partial Z$), seismic attenuation ($\partial Q/\partial Z$), bulk compressibility ($\partial\beta/\partial Z$), bulk thermal conductivity ($\partial\bar{K}/\partial Z$), *in-situ* fluid permeability (gas, water, magma) ($\partial K_f/\partial Z$), and electrical resistivity ($\partial\Omega/\partial Z$), as well as the predictions of volumetric strain for jointed media (RYAN, 1985; 1987), demonstrate that this dependence will be non-linear.

Studies of the three–dimensional distribution of seismicity at Kilauea provide an additional means of evaluating the depth distribution of magma associated with subcaldera storage (RYAN *et al.*, 1981). These results may be summarized in vertical profiles taken beneath the caldera as well as beneath Halemaumau (RYAN *et al.*, 1983), (Figure 7a). From

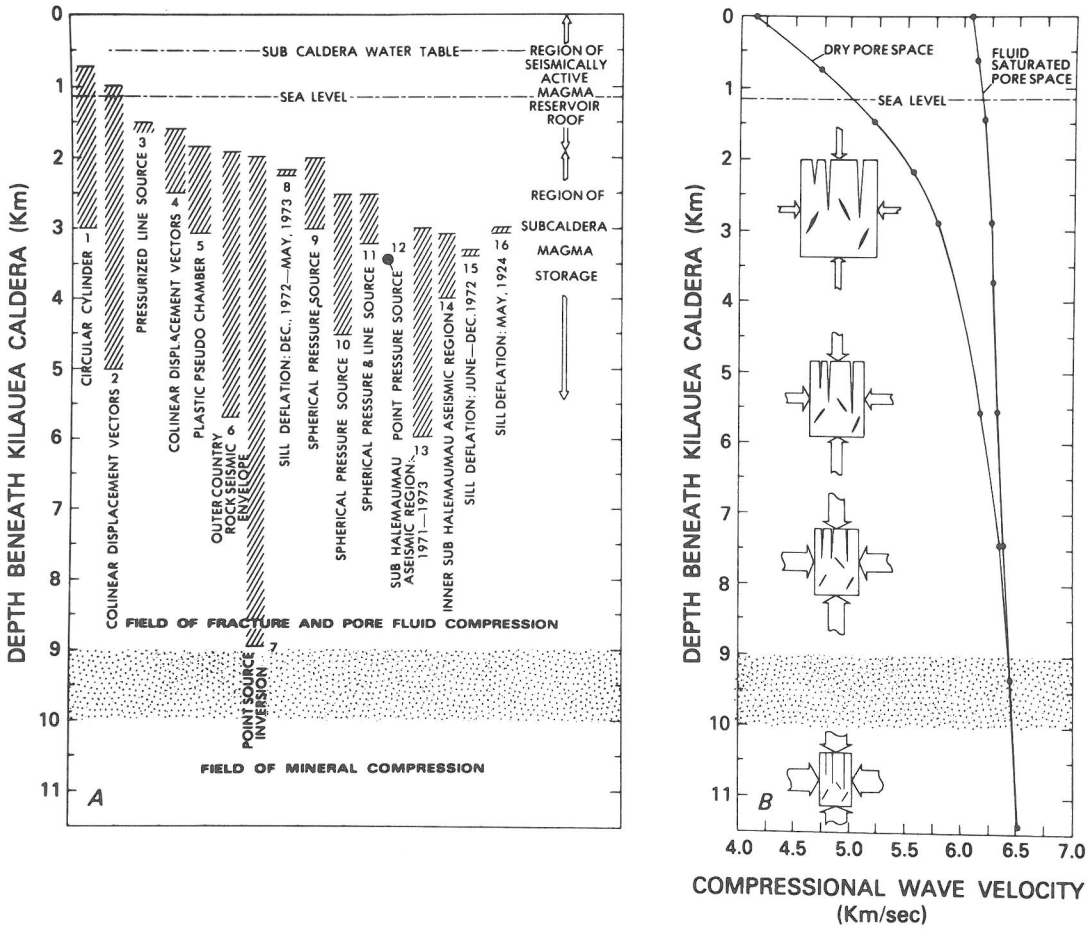

FIG. 6a, b. (A) The depth range of subcaldera magma storage for Kilauea, as inferred from geodetic and seismic surveys. The total range for a given survey is given by the vertical cross-ruled band. The identity of the source model geometry and the theoretical inversion or forward modeling procedure is given beneath each inferred magmatic interval. Respective source references are: (1) DIETERICH and DECKER (1975); (2) DUFFIELD *et al.* (1982); (3) WALSH and DECKER (1971); (4) MOGI (1958); (5 and 7) JACKSON *et al.* (1975); (6) FISKE and KINOSHITA (1969); (8) DAVIS *et al.* (1974); (9) RYAN *et al.* (1981); (10) DVORAK *et al.* (1983); (11, 14, 15 and 16) RYAN *et al.* (1983); (12) EATON (1962); and (13) KOYANAGI *et al.* (1976). (B) The compressional wave velocity for dry and seawater saturated basalt as a function of depth-equivalent confining pressure. The interval 0–9 km corresponds to the confining pressure required for the closure of fluid accessible pore space in the absence of an applied pore pressure. Block diagrams schematically illustrate the progressive closure of the macroscopic and microscopic fracture networks as confining pressures are progressively increased. The convergence of the dry and H_2O–saturated V_p branches at a 9–10 depth equivalent, separates the upper field of fracture and pore fluid compression from the lower field of mineral compression. The stippled band is the contractancy transition zone. V_p data from CHRISTENSEN (1974) and CHRISTENSEN and SALISBURY (1975). Figure modified from RYAN (1987).

0 to 2 km depth, intense seismicity is produced by the flexure of the storage complex roof; from 2 to 7 km, an increasingly aseismic region attests to relatively high fluid-to-rock ratios, with the interval 4 to 7 km being very aseismic; at depths in excess of 7 km, the intensity of hydraulic fracturing rises, suggesting the active vertical transport of magma within the dikes that make up the primary conduit.

In Figure 7b, the *in-situ* densities of Kilauea and Mauna Loa have been compiled from the gravity inversion studies of ZUCCA *et al.* (1982). These correspond to both summit and flank profiles for each volcanic shield. For both volcanoes, the density profiles increase in a non-linear manner with depth from 0 to 7 km. This band generally corresponds with the non-linear portion of the experimentally-

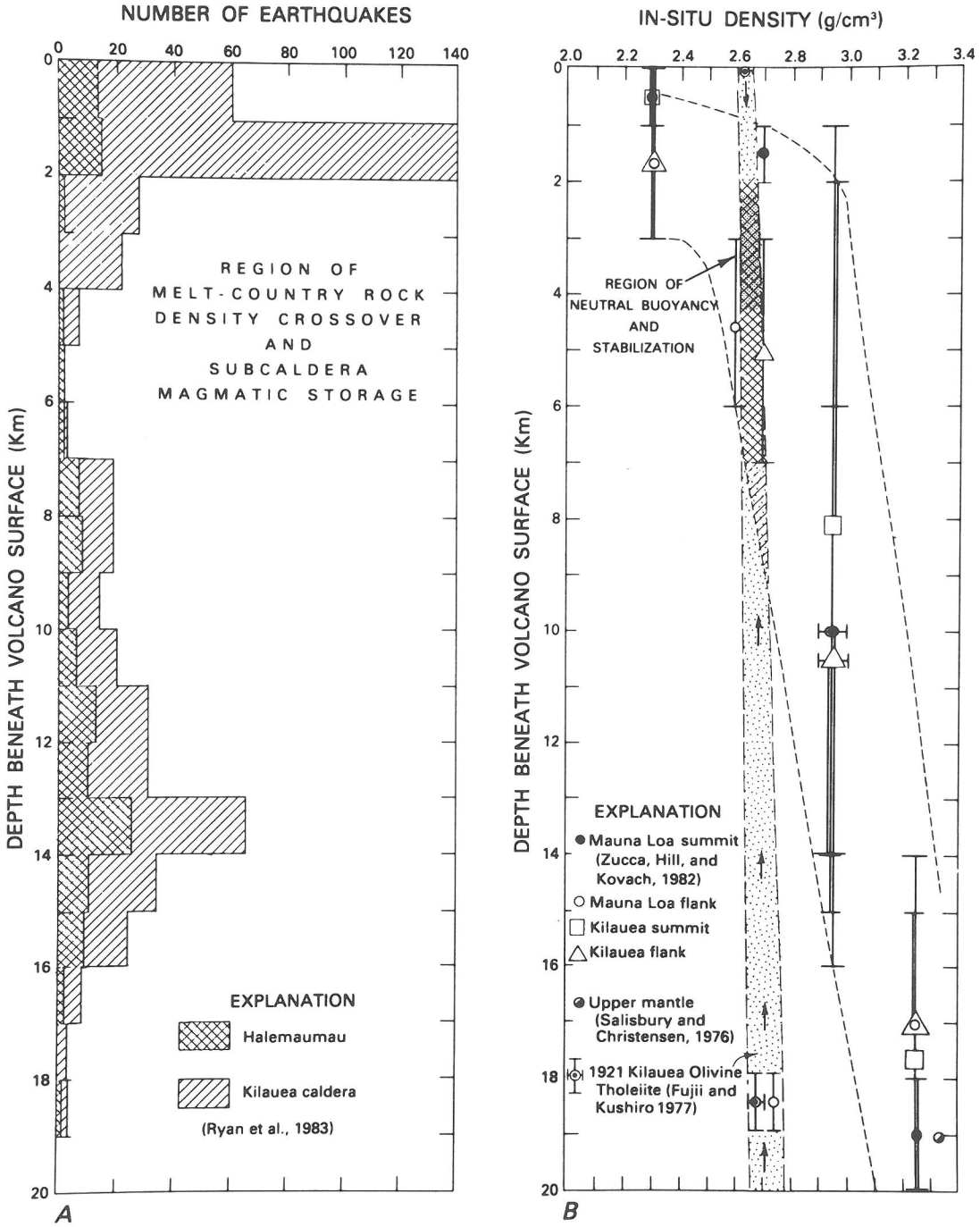

FIG. 7a, b. (A) The representative depth distribution of the rate of earthquake occurrence for two prismatic volumes of Kilauea volcano. Both volumes extend to 20 km beneath the caldera floor; however, one volume is laterally extensive, and contains the entire caldera (single cross-ruled pattern). The second volume is focused on Halemaumau crater within the caldera, and it's substructure (double cross-ruling). In both cases, an aseismic region extends from 4 to 7 km, suggesting differentially high magma to countryrock ratios within the summit storage reservoir. For the immediate substructure of Halemaumau, this region extends from 2 to 7 km. The interval 2 to 4 km is the most frequently retrieved storage depth from geodetic studies, as illustrated in Figure 6a. (B) *In-situ* density values and their depth ranges as derived from the gravity inversion study of the summit and flanks of Kilauea

based contractancy curves for basalt and gabbro (Figures 2, 3). In addition, the band corresponds closely with the 0–9 km depth range necessary to achieve a convergence in the air-saturated and H_2O–saturated branches of the V_p vs. confining pressure ($P_{conf.}$) profile in Figure 6b.

Moreover, there is additional congruence between the non-linear variation in contractancy-related material properties associated with the Earth's surface: the systematics of the *in-situ* change in compressional wave velocity for Hawaii based on the seismic refraction surveys of HILL (1969); and the compilations of WARD and GREGERSEN (1973), CROSSON and KOYANAGI (1979), and KLEIN (1981). These velocity profiles are assembled in RYAN (1987) and are compared and contrasted with the $\partial V_p/\partial Z$ for basalt, gabbro, peridotite, and dunite, which represent the lithologies of the volcanic shields, oceanic crust, upper mantle and refractory path regions of the tholeiitic suite of magmas. These results suggest that several physical states and derivative properties—*in-situ* densities, *in-situ* compressional wave velocities, laboratory-derived V_p and V_s, and field studies of gravity are all responding to the non-linear contractancy associated with the Earth's surface; that is, the progressive elimination of void space on all scales with depth. Figure 8, based on the seismic refraction survey of ZUCCA *et al.* (1982), summarizes the two-dimensional velocity structure for the traverse from Mauna Loa to western offshore Hawaii. Attention is drawn to the very low V_p values of the highly porous surficial veneer and to the velocity values suggestive of gabbro and gabbro + dunite mixtures within the core of Mauna Loa. This last region is labeled 'intrusive complex' in the figure.

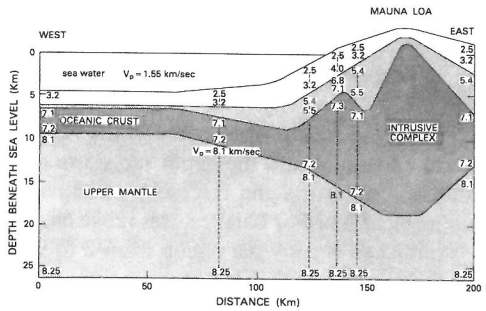

FIG. 8. Seismic velocity structure of the island of Hawaii along a profile linking the Mauna Loa substructure with west and offshore Hawaii. Compressional wave velocities (in km/sec) along six vertical profiles, as inferred from refraction survey travel time data, are the numbers linked by dashed lines. Attention is drawn to the high velocity core region of Mauna Loa's intrusive complex, and to the very low velocities deduced from the surficial veneer of fracture basalt and hyaloclastite. Modified from ZUCCA *et al.* (1982).

NEUTRAL BUOYANCY AND MAGMA STABILIZATION

The density of the 1921 Kilauea olivine tholeiite has been measured over the pressure range 0.1 MPa to 1500 MPa, at temperatures of 1250 to 1400°C by FUJII and KUSHIRO (1977). These results have been incorporated in Figure 7b. Attention is drawn to the cross-over in melt and countryrock density—a cross-over produced by the low *in-situ* density of the heavily fractured veneer that makes up the upper 2 to 3 km of the volcanoe's superstructure. *Within the core of the cross-over region lies a subregion of density equilibration between the melt and countryrock. This is referred to as the region of neutral buoyancy and magma stabilization.*

Magma arriving in Kilauea's summit reservoir has been estimated to contain about 0.32 weight percent H_2O (GREENLAND *et al.*, 1985), in broad accord with MOORE's (1965) estimate of 0.45 ± 0.15 weight percent H_2O for deep sea Hawaiian basalts. KUSHIRO (personal communication, 1986) has measured the density change produced by the addition of 1.08 weight percent H_2O to a basaltic melt, and finds a decrease of 0.05 g/cm^3 compared with the anhydrous liquid. This represents an upper limit for the expected effect of dissolved H_2O. For all

and Mauna Loa volcanoes. The vertical extent of the bars delimit the depth range for *in-situ* densities, whereas the central circles, squares and triangles correspond to vertical profiles beneath Mauna Loa's or Kilauea's summit or flank. The combined results suggest a non-linear *in-situ* density vs. depth profile. Superposed on the countryrock density profile is the pressure (depth) dependence of density for the 1921 Kilauea olivine tholeiite (stippled band), from the falling sphere densitometry experiments of FUJII and KUSHIRO (1977). An *in-situ* cross-over region occurs in the 1 to 7 km depth interval. Within the heart of this interval is a subregion of inferred neutral buoyancy and magma stabilization, that has a 1:1 correspondence with the 2 to 4 km depth interval associated with summit magma storage—for both Kilauea and Mauna Loa volcanoes. Upward-directed arrows in the lower portion of the stippled band suggest magma motion directions in response to positive buoyancy. The downward–directed arrow at top of band suggests the motion direction for negative buoyancy. *In-situ* density values are from the study of ZUCCA *et al.* (1982). Figure modified from RYAN (1987).

conceivable H_2O contents for these tholeiitic melts, therefore, the small density perturbation would be well within the stippled melt density band of Figure 7b.

What is the relationship between the region of neutral buoyancy, and the depth range associated with the summit magma reservoirs of active Hawaiian volcanoes? For Kilauea, this range has been constrained to occupy the region from 2 to 9 km, with the subrange 2 to 4 km representing the consensus of nearly thirty years of geodetic study (MOGI, 1958; EATON, 1962; FISKE and KINOSHITA, 1969; WALSH and DECKER, 1971; DIETERICH and DECKER, 1975; JACKSON *et al.*, 1975; SWANSON *et al.*, 1976; DUFFIELD *et al.*, 1982; RYAN *et al.*, 1983; DVORAK *et al.*, 1983; DAVIS *et al.*, 1974; and DAVIS, 1986). With respect to the *in-situ* density cross-over region of Figure 7b, the core of neutral buoyancy occupies the 2.5 to 4.5 km depth levels. This suggests a remarkable correspondence between the depths at which magma is in approximate mechanical equilibrium with its surroundings and the region independently demonstrated to comprise Kilauea's subcaldera magma storage region. A further comparison of the overall 2 to 7 km interval (Figure 7) shows additional congruence: there is a 1:1 correlation between the region associated with subcaldera magma storage, and the region of magma-country rock equilibrium inferred from the equality of *in-situ* melt-rock densities.

THE MECHANICS AND DYNAMICS OF NEUTRAL BUOYANCY

Consider the steady, low velocity influx of melt, rising vertically into a magma reservoir, and having an initial density ρ_0, that is different from the ambient density, ρ_a. Due to the density contrast, the fluid exiting the conduits that supply the base of the magma reservoir is subject to buoyancy forces.

If the environmental density progressively decreases upwards—in either a linear or non-linear pattern—the ambient medium is referred to as 'stably stratified' (FOX, 1970; HIMASEKHAR and JALURIA, 1982; HIRST, 1971). Rising melt batches then undergo a continuous reduction in their buoyancy flux, until it eventually approaches zero. This region is the 'point of neutral buoyancy'. Above this point is the region of negative buoyancy ($\rho_{melt} > \rho_{environment}$), and the flow decelerates markedly, where its velocity falls to zero at the maximum height of rise (JALURIA, 1986). After reaching the peak height, fluid parcels descend, spreading outwards towards a laterally-extensive horizon of neutral buoyancy. Along this horizon, they further mix with the ambient fluid (RODI, 1982; HUPPERT *et al.*, 1986).

In the discussion above it has been assumed that the melt has a density that interacts with the far–field host rock environment of the volcanic shield or the near-field 'host fluid' environment of the reservoir itself. Melt density, however, will exhibit a temperature and time dependence during fractional crystallization, which will lead to a set of embedded systems: the large-scale system of the reservoir as a whole, as it interacts with the surroundings on a scale of several kilometers, and an embedded, smaller-scale subsystem described by the dynamics of individual melt parcels and the ambient fluid that forms their immediate environment.

With the data of BENDER *et al.* (1978), MCBIRNEY and AOKI (1968), SHIBATA *et al.* (1979), and WALKER *et al.* (1979) from 0.1 MPa experiments and residual glasses of basalts from oceanic islands and mid-ocean ridge basalts (MORB), STOLPER and WALKER (1980) recognized that the fractional crystallization of a picritic melt leads to progressive changes in the density of the remaining liquid. Olivine removal (with or without concurrent clinopyroxene (cpx) crystallization) reduces the density of the residual melt. The extreme range was a reduction of ≈ 0.1 g/cm^3; however, HUPPERT and SPARKS (1980) suggested a decrease of ≈ 0.2 g/cm^3 for the picritic basalt-to-MORB minimum point. Subsequent comparisons of measured 'fractionation densities' and densities calculated by a weighted average mixing procedure (SPARKS and HUPPERT, 1984), suggest that, while numerically small, the effect is real.

At the magma reservoir margins and beneath the rift system axes, the horizon of neutral buoyancy is coincident with the peak in the available magma driving pressure—that pressure required to do the work of rock fracture at the propagating dike formation front. This occurs regardless of the depth of origin of the magma, variations in magma density, or the stratigraphic details of where in the overlying section the final density balance is achieved.

Consider the differences in pressure between a lithostatic and magmatic column as a function of magma density and with provision for a non-linear distribution of countryrock densities in the near-surface. The driving pressure, P_d, at a given height above its source, h, is (*e.g.*, JOHNSON and POLLARD, 1973):

$$P_d = P_m - P_L, \tag{1}$$

$$P_d = P_m - \rho_{CR} G \bar{H}, \tag{2}$$

$$P_d = (P_s - \gamma_m h) - \rho_{CR} G \bar{H}, \quad (3)$$

where P_m is the magma pressure, P_L is the lithostatic load, γ_m is the unit weight of the magma, and P_s is the lithostatic pressure in the source region. The lithostatic load is

$$P_L = \rho_{CR} G \bar{H}, \quad (4)$$

where $\bar{H}$ is the depth beneath the upper reference surface, and ρ_{CR} is the countryrock density. Curves of P_d vs. depth (*e.g.*, JOHNSON and POLLARD, 1973, p. 284; FEDOTOV, 1977, p. 677) have a characteristic parabolic profile for conditions of increasing pressure (P_L) with depth if and only if the near surface veneer has an *in-situ* density lower than the magma. The nose of the driving pressure parabola then lies at the depth at which $\rho_{magma} \cong \rho_{countryrock}$, that is, the neutral buoyancy surface. It is interesting to note that in terms of the mechanical and transport properties of a subcaldera magma reservoir and of active rift systems the peak in magma driving pressure coincides with that depth at which rock moduli and strength-related parameters (*e.g.*, V_p and V_s) begin a marked fall-off (Figures 2–5 and BRACE, 1971b; BYERLEE, 1968), whereas fluid-accessible permeability (k_f) begins a corresponding marked increase. This is the region of neutral buoyancy. It is then no surprise that rupture of the magma reservoir walls should occur over and over again at the same preferred depth, as discussed below.

How does the region of neutral buoyancy control the magma injection-dike formation process, and what is its mechanical signature? Earthquake hypocenters produced by the hydraulic fracturing associated with magma injection and dike formation in rift zones provide a means of answering these questions. Hypocenters have been determined for Kilauea's Southwest and East Rift Zones. By plotting their locations on a depth-time diagram (Figure 9), temporal variations in the top and the keel of a growing dike may be inferred. In addition, the relationship of the region of neutral buoyancy to the point of dike initiation, the centerline axis of dike symmetry, the depth position of the advancing dike snout and the final resting place of the leading magma fracture front may all be determined from hypocenter data.

Figures 9a through 9f present a series of depth-time dike propagation envelopes for both of Kilauea's rift zones. They show the following general characteristics: at the moment of summit reservoir rupture and rift zone intrusion, reservoir breaching occurs by failure of the confining wall rock at the depth of the region of neutral buoyancy. This region is centered at the 3 km depth level, beneath the caldera floor. Rift zone intrusion occurs by the lateral propagation of a magma-filled fracture, along the horizon of neutral buoyancy. Propagation continues until the fluid pressure falls below that required to meet and exceed the *in-situ* tensile strength of host rock at the advancing magma fracture front.

In detail, three modes of neutral buoyancy-controlled dike formation have been recognized. (1) Slow initial leakage with a gradually enlarging magma fracture front as illustrated by results shown for Kilauea's east rift zone in Figure 9a. Initiated along the horizon of neutral buoyancy, the growing dike has a top that rises progressively towards the surface, while the keel simultaneously descends. The intrusion may end abruptly (Figure 9a), forming a cross-sectional depth-time signature that resembles a tomahawk head, with the blade facing down-rift. (2) Abrupt initial leakage with a rapidly enlarging magma fracture front. Here, the top of the dike grows rapidly towards the surface, while the keel simultaneously (and rapidly) descends (Figure 9b). Subsequent inferred pressure reductions gradually narrow the advancing fracture front, and inferred positive and negative buoyancy forces return parcels of magma below and above the horizon of neutral buoyancy, to positions of mechanical equilibrium. The resting place of the dike snout after growth has been completed is thus along the horizon of neutral buoyancy. The depth-time signature therefore resembles an up-rift facing tomahawk (Figure 9b). (3) Harmonic oscillations of the top and keel of the growing dike (Figures 9c–9f). Here, the intrusion is again initiated within the region of neutral buoyancy, and the top and bottom of the extending dike antithetically rises and falls together as time progresses. The resulting depth-time signature resembles a knife blade with doubly-serrated edges: the valleys and hills on each "edge" of the dike face each other on either side of an axial plane of bilateral symmetry. For Kilauea, this type of harmonic neutral buoyancy-controlled dike growth occurs within both rift zones. Amplitudes of the rising and falling tops and keels vary from $\approx$2 to 3 km (Figures 9a and b) to $\approx$6 km (Figure 9d). Periods of the harmonic fracture process vary from $\approx$6 hrs. (Figure 9c), to 78 hrs. (Figure 9f). In all cases (types (1), (2) and (3)), the horizon of advance corresponds to the depth horizon of neutral buoyancy. Above and below this level, magma rises and falls in vertical expansion and contraction pulses, corresponding to the momentary buildup of inferred pressure differentials within the momentarily stalled dike.

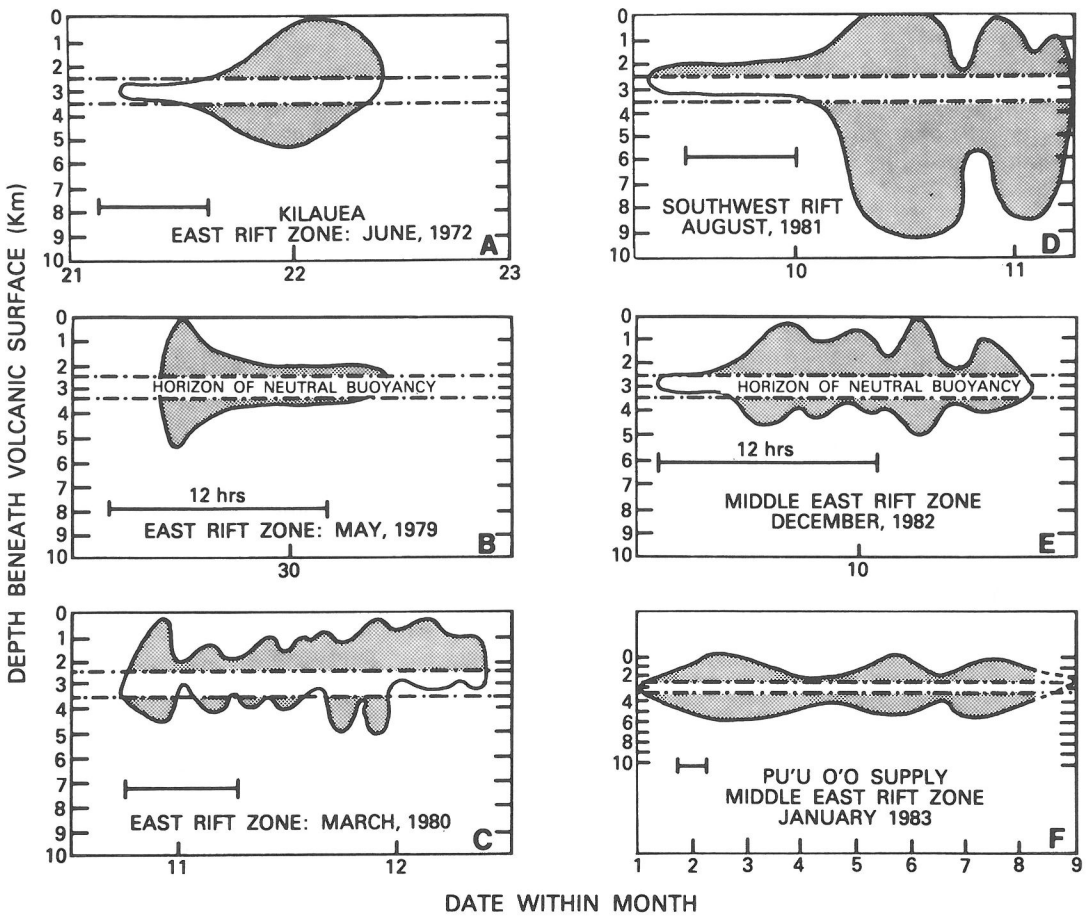

FIGS. 9a–9f. The time variation in the vertical extent of magma during rift zone intrusion at Kilauea volcano, Hawaii. These envelopes, in depth-time plots, enclose the cross-sectional upper and lower limits of the seismicity associated with the magmatic fracture and dike formation process, and have been constructed from the compilation in KLEIN *et al.* (1987). The horizontal stippled band corresponds to the horizon of neutral buoyancy, where the in-situ $\rho_{melt} \approx \rho_{countryrock}$. In the frames, the relevant time periods are: (9a) June 21–23, 1972; (9b) May 29–30, 1979; (9c) March 10–12, 1980; (9d) August 9–11, 1981; (9e) December 9–10, 1982; and (9f) January 1–8, 1983. The datum for the depth is the Earth's surface above the seismic swarm produced by rising magma pressure. Particularly striking throughout this sequence of frames, is the marked symmetry of the vertical extent of magma about the horizon of neutral buoyancy. In all cases, the horizontal bar represents 12 hours.

Achieving the requisite pressure to exceed the critical stress intensity factor (K_{Ic}) required for dike advance, then reduces this inferred pressure level, extends the dike, and produces a "necking" (narrowing) in the vertical extent of the magma fracture front. The cycle is then repeated.

Figure 10 illustrates the three–dimensional internal structure of Kilauea with respect to primary magma transport routes and the horizon of neutral buoyancy. The model has been constructed by integrating seismic constraints (RYAN *et al.*, 1981; RYAN, 1987) with the continuum mechanics of the magma transport process, combined with the results of geodetic surveys and the structural and eruptive geology of the volcanic shield.

After ascent through the primary conduit, magma stored within the summit reservoir is periodically injected laterally into the rift zones, in dike formation episodes. This may take the form of discrete dikes whose rear is connected to the reservoir structure, or the transfer of magma batches, to still-molten regions of rift zone storage, as occurred during the Pu'u O'o eruptive sequence. Because of the tendency for magma to be both stored and transferred

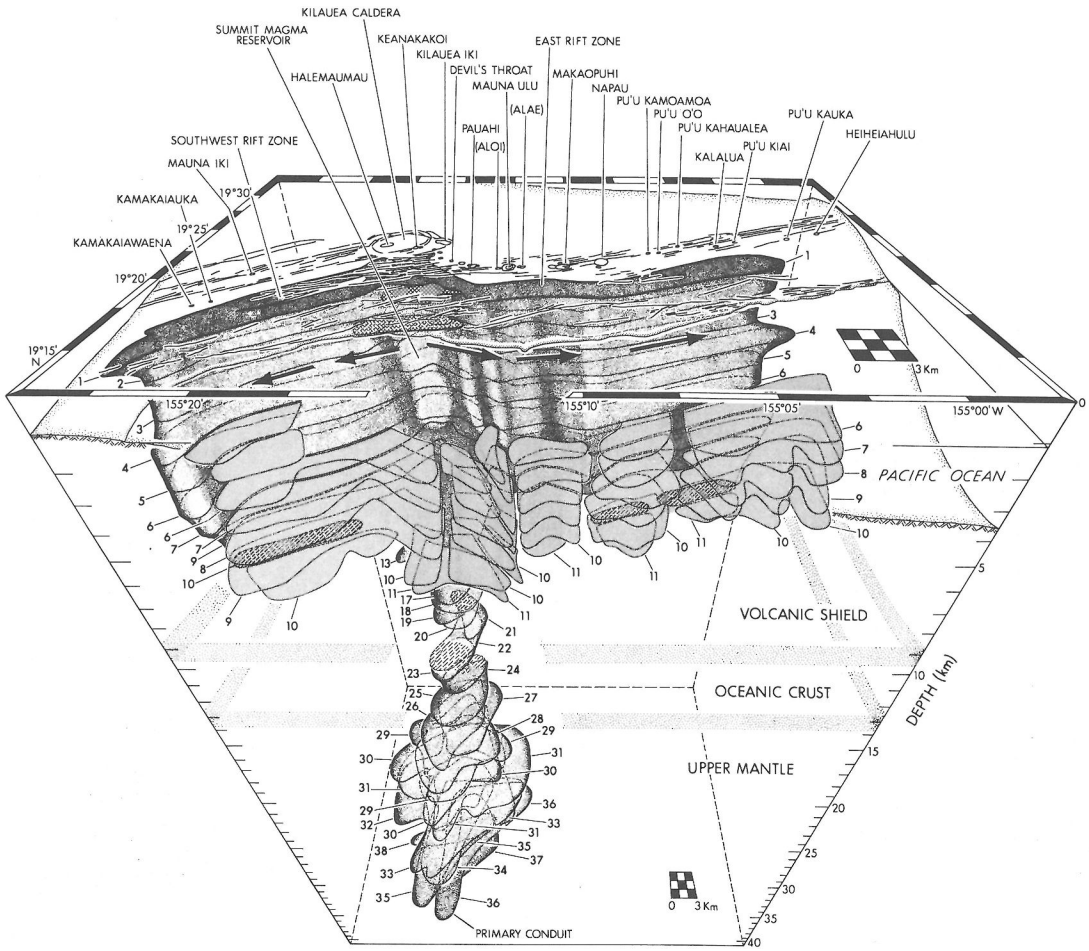

FIG. 10. The three–dimensional internal structure of Kilauea volcano, in a northward-directed view. The medium stippled pattern denotes the substructure of the southwest and east rift zones, that radiate from the summit magma reservoir, as well as the primary conduit, rising from a depth of 40 km into the base of the reservoir. The reservoir appears as a lightly-shaded central region with an overall depth extent of 2 to 7 km, whose upper levels lie behind the tectonic blocks of the Koae Fracture System (cross-hatched pattern) from this perspective. The rift zones lie behind the seismically active tectonic blocks of the south flank (medium grey pattern). The periodic high level injection of magma into the rift zones occurs along the horizon of neutral buoyancy (arrowed pathways) and is associated with the lateral formation of dikes at the ≈3 km local reference level beneath the volcanic surface. Figure modified from RYAN (1987).

within the horizon of neutral buoyancy, magma mixing in active volcanic systems is expected to occur preferentially within this horizon.

NEUTRAL BUOYANCY AND THE EVOLUTION OF HAWAIIAN SHIELD VOLCANOES

The zero confining pressure datum for the contractancy profile of a subaerial volcano is, of course, positioned at the Earth's surface. For submarine volcanoes, this will correspond to sea level, because the weight of the superjacent column of seawater will contribute to the compressive stress exerted across vertically-oriented planes within the seamount, and in the oceanic crust beneath. During the growth of a Hawaiian shield, the dilatant fracture network associated with the Earth's surface (free surface reference level) produces a contraction profile. For subaerial volcanoes, the profile's datum is the caldera floor, or the rift zone crest; that is, that portion of the Earth's surface directly above the intrusive complex of interest. An increase in depth

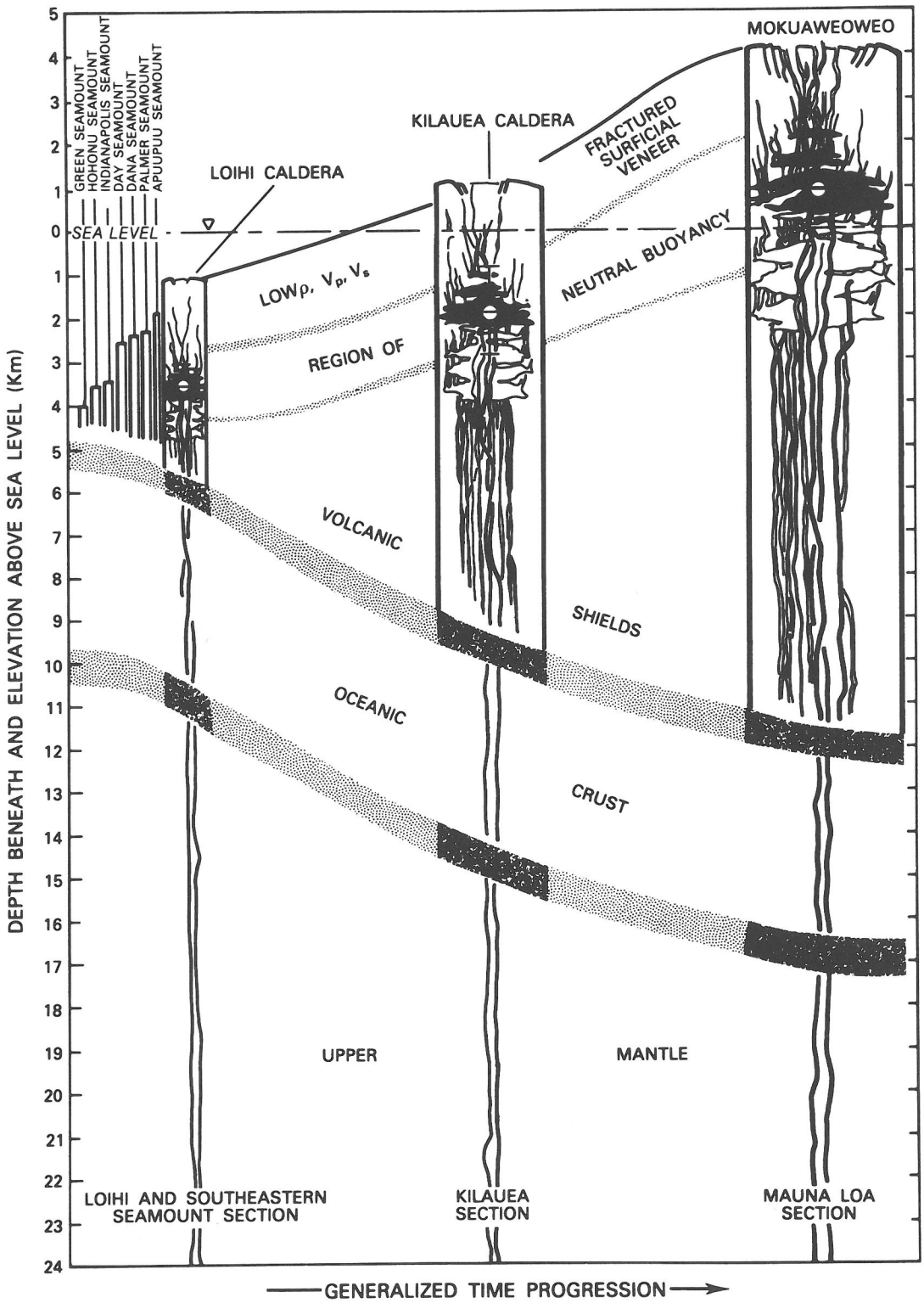
GREEN SEAMOUNT
HOHONU SEAMOUNT
INDIANAPOLIS SEAMOUNT
DAY SEAMOUNT
DANA SEAMOUNT
PALMER SEAMOUNT
APUUPUU SEAMOUNT
LOIHI CALDERA
KILAUEA CALDERA
MOKUAWEOWEO
FRACTURED SURFICIAL VENEER
SEA LEVEL
LOW ρ, Vp, Vs
REGION OF
NEUTRAL BUOYANCY
VOLCANIC
SHIELDS
OCEANIC
CRUST
UPPER
MANTLE
LOIHI AND SOUTHEASTERN SEAMOUNT SECTION
KILAUEA SECTION
MAUNA LOA SECTION
DEPTH BENEATH AND ELEVATION ABOVE SEA LEVEL (Km)
GENERALIZED TIME PROGRESSION

produces an increase in confining pressure—first squeezing shut the dilatant and permeable fracture space, then, beneath the contractancy transition zone—compressing the minerals of the rock matrix. *It is therefore the depth beneath the free-surface reference level that regulates the amount of intrinsic dilatant fracture permeability in shallow portions of volcanic systems. Raising the free surface, therefore, progressively raises the contractancy transition region within the system.* In simpler terms, as a volcano grows upward, it carries its contractancy profile with it.

Inside a given magma storage complex, the region of neutral buoyancy will regulate the positioning of the upper levels of the stable reservoir, whereas the lower basal levels will be ordered by the final squeezing shut of the fracture permeability associated with passage through the contractancy transition zone. *In an almost a literal sense,* Hawaiian magma reservoirs lift themselves by their own "boot straps": *the addition of eruptive products to the top of the system, progressively raises all the critical reference levels within the system—the zero confining pressure datum, the horizon of neutral buoyancy, and the contractancy transition zone. The summit storage reservoir and its associated rift systems must now elevate themselves to achieve mechanical equilibrium within the shield.* Thus, the life cycle of Hawaiian magmatism is controlled by an evolutionary track along which the fluid regions of active storage and differentiation are continuously squeezed upwards. Only a reduction or curtailment of the supply at depth can slow or stop this evolutionary process. Figure 11 illustrates the evolution and upward growth of a Hawaiian volcanic shield, from the initial stage of submarine activity, through subaerial growth to relative inactivity in the waning stages of subaerial development. It represents the vertical progression illustrated topographically in Figure 1. In the terms of Davisian geomorphology, these three evolutionary stages would be submarine infancy, subaerial maturity and subaerial old age, respectively.

NEUTRAL BUOYANCY AND ICELANDIC MAGMATISM

The remarkable correlations between regions of intra-shield magma transport and storage for Hawaii and the relevant physical properties of basic and ultrabasic rocks and melts suggests that we look beyond Hawaii for similar correlations. Encouraged by the essential simplicity of the rift zone intrusion process, we next turn our attention to the north of Iceland and the current eruptive episode at the Krafla central volcano and its associated rift systems (Figure 12).

The depths of subcaldera magma storage at Krafla have been studied through three general approaches: (1) seismic shear wave attenuation patterns (EINARSSON, 1978); (2) inversion modeling of caldera displacement and tilt patterns (BJÖRNSSON *et al.*, 1979; TRYGGVASON, 1981, 1986; MARQUART and JACOBY, 1985); and (3) forward modeling of magma withdrawal from sills combined with a collateral study of exhumed intrusives in the Tertiary central volcano complexes of eastern Iceland and adjunct seismic constraints (RYAN, in preparation). Figure 13 summarizes the depth intervals suggested for Krafla magma beneath the central caldera. The total range is 2.5 to 7.0 km, with the sub-interval 2.5 to 4.0 km representing that range common to all nine studies. As in the Hawaiian context, the geodetic surveys emphasize the upper levels of the storage region. In a companion plot, Figure 14 presents a depth comparison for Krafla's rift systems, where the total interval is 1.0 to 5.75 km, and the subinterval 1.0 to 3.5 km is the most frequently retrieved depth range for dike formation.

The compressional wave velocity profile for the Icelandic crust is a nonlinear but continuous in-

FIG. 11. The nature of the evolutionary track during the growth and development of oceanic volcanoes. The volcanic shield-oceanic crust interface is stippled and is isostatically depressed under the volcanic load. As a volcano grows and evolves, it carries its contractancy profile with it. Concomitant changes along this evolutionary track include: (1) a progressive upward migration in the transition zone that separates the fields of fracture and pore fluid compression above, from mineral compression below (not illustrated); (2) a progressive upward migration of the zone of neutral buoyancy (circle with horizontal dash); and (3) a progressive elevation of the fractured surficial veneer, with its characteristic non-linear mechanical and transport properties. This provides the mechanical rationale for the evolutionary climb of subcaldera magma reservoirs in the progression from submarine activity (infancy) (A), to the waning stages of development (subaerial maturity) (C). The crustal structure and the volcanic shield-oceanic crust and oceanic crust-upper mantle transition zones have been constrained by the studies of HILL (1969), ZUCCA and HILL (1980) and ZUCCA *et al.* (1982). Active magma reservoirs and their dike systems are illustrated in black. Inactive reservoirs and their dikes are white. Only the most recent generation of inactive reservoirs has been shown. Seamounts adjacent to the island of Hawaii have been ranked by their summit depth below sea level.

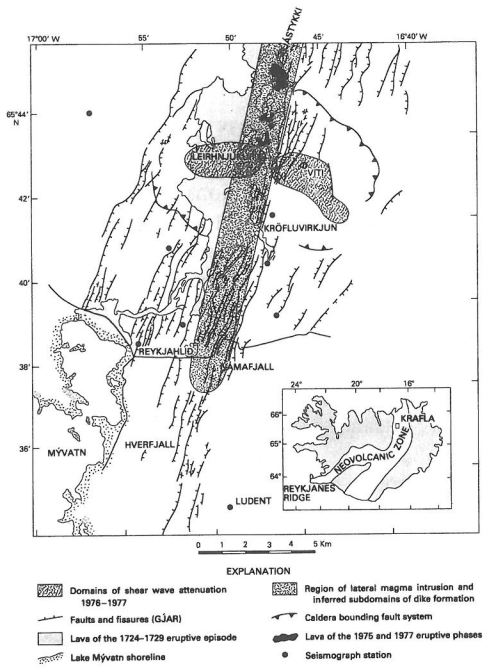

FIG. 12. The juncture of the caldera and the rift systems associated with the Krafla central volcano, northeast Iceland. Magma accumulates beneath the caldera floor in the region of neutral buoyancy prior to the initiation of intrusive and eruptive activity. Intrusion south-southwestward into the Námafjall rift system or north-northeastward into the Gjástykki rift system is guided by the topography of the horizon of neutral buoyancy—inferred to lie at a local depth of 2 to 4 km beneath the volcano's surface. It is also postulated to descend slightly towards the north and south, mimicking at depth the general surface topography of the volcano. Domains of shear wave attenuation are from EINARSSON (1978) and occur beneath the caldera. The region of lateral magma intrusion and inferred dike formation is based on the seismic and geodetic surveys of EINARSSON and BRANDSDOTTIR (1980), TRYGGVASON (1984, 1986) and BJÖRNSSON *et al.* (1979). (Modified after the structural sketch map of K. Saemundsson, in BJÖRNSSON *et al.*, 1979.)

crease in V_p with depth (FLOVENZ, 1980). The lowest velocities are above the water table, in the near-surface of the neovolcanic zone ($\approx$2.0–2.5 km/sec), and reach $\approx$6.5 km/sec at a depth of about 6 km (FLOVENZ *et al.*, 1985). Part of this non-linear increase is ascribed to the progressive closure of fractures, whereas part is ascribed to secondary minerals and the progressive metamorphism of the crust (CHRISTENSEN and WILKENS, 1982). In regions of active volcanism, we should expect to see a constant competition between the hydrothermal alteration and secondary mineralization processes that tend to seal fractures, and the pervasive cracking process associated with magmatic movement and dike emplacement—creating new fracture networks and dilating preexisting cracks. In this report, the transition from non-linear to linear increases in V_p, occurring at a depth of 6 km within the volcanic zone, is taken to represent the region of transition from fracture and pore fluid compression to deeper mineral compression (FLOVENZ, written communication, 1986). It corresponds closely with the lowest levels of inferred magmatic storage beneath Krafla caldera (Fig. 13), and lies at or beneath the inferred keels of rift zone dikes as illustrated in Figures 14 and 15.

Stimulated by the strong similarities in the depth ranges for magma within the upper levels of the Hawaiian and Icelandic volcanic systems, we now inquire about the existence of regimes of neutral buoyancy in Iceland. A summary of the geologic nature and density of Icelandic crustal layers is given in Table 1. Particularly noteworthy are inferred densities in the range 2.1 to 2.5 g/cm^3, that characterize the uppermost $\approx$1000 m. Lithologically,

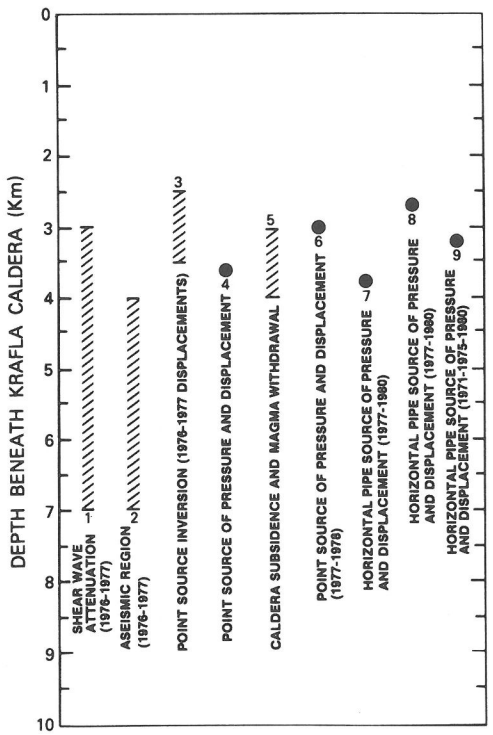

FIG. 13. Depth of subcaldera magma storage at the Krafla central volcano, northeast Iceland. The data and inversion modeling references are (1 and 2) EINARSSON (1978); (3) BJÖRNSSON *et al.* (1979); (4) TRYGGVASON (1981, 1986); (5) M. P. RYAN, unpublished numerical results (1983); (6) JOHNSEN *et al.* (1980); (7, 8 and 9) MARQUART and JACOBY (1985). Dots represent discrete inferred depths.

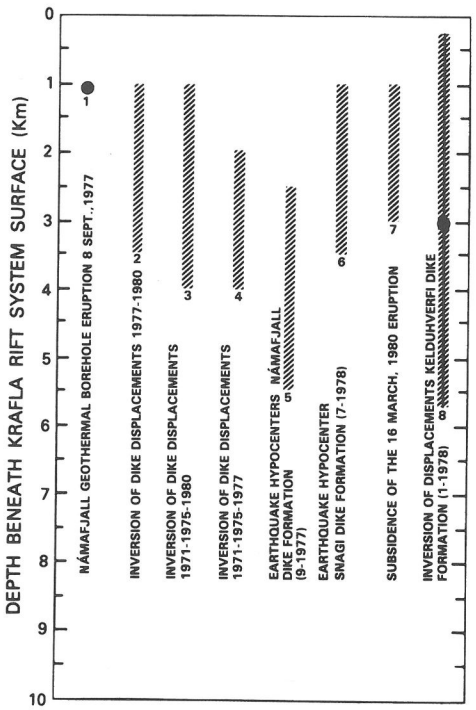

FIG. 14. Depth and inferred depth ranges of rift system dike formation during lateral magma injection pulses at the Krafla central volcano. The data and inversion modeling references are: (1) BJÖRNSSON and SIGURDSSON (1978); LARSEN *et al.* (1979); (2, 3 and 4) MARQUART and JACOBY (1985); (5 and 6) BRANDSDÓTTIR and EINARSSON (1979); (7) TRYGGVASON (1980); and (8) POLLARD *et al.* 1983).

this is a heavily fractured layer of basalts, hyaloclastic breccias, and tuffs. Beneath lie the progressively altered basalts of layer 1, with densities of about 2.60 g/cm^3, and an average estimated thickness of $\approx$1000 m. Still deeper are flood basalts that have been locally intruded with gabbroic and granophyric masses. Here the *in-situ* density is $\approx$2.65 g/cm^3, and the average thickness is estimated at $\approx$2100 m. This comprises crustal layer 2. Recalling that the experimentally determined density of tholeiitic melt above its liquidus is 2.62 g/cm^3 (FUJII and KUSHIRO, 1977), two conclusions may now be drawn: (1) a region of neutral buoyancy exists within the heavily fractured neovolcanic zone, and is constrained to lie at a depth of 2 to 4 km; and (2) the presence of masses of gabbro and granophyre suggest that the upper levels of Icelandic magma reservoirs occur within layer 2; that is, these intrusive complexes record the fossil zone of neutral buoyancy, and their emplacement was regulated by it. WALKER (1974, 1975) also recognized the equity in density between magma and high levels of the Icelandic crust, and suggested that sheet intrusions may, in part, be controlled by this balance.

A summary of the dynamics and kinematics of the current tectonic episode at the Krafla central volcano illustrates the role of neutral buoyancy within a spreading center context. Following the Mývatn Fires (Mývatnseldar) rifting and eruptive episode of 1724–1729, the Krafla region lay quiet until December, 1975. Eruptive and intrusive activity then resumed in a series of 9 eruptions and 12 intrusions that injected magma both north and south of the central caldera (Figure 12). During these periods of lateral rift zone magma injection, the volcanic surface surrounding Leirhnjúkur—a horst-like hyaloclastite ridge studding the topographic high of Krafla's caldera floor—subsided as much as 230 cm, in response to withdrawn magma volumes of 130 $\times$ 10^6 m^3 (JOHNSEN *et al.*, 1980; BJÖRNSSON, 1985). The breaching of the reservoir wall rock at depths of 2 to 4 km periodically released batches of magma during dike-forming intrusive episodes. The seismicity associated with these intrusions, when viewed as a time progression during the course of hydraulic crack propagation in vertical cross-section, allows one to keep track of the evolving geometry of the magmatic fracture front, and, by inference, the evolution of the lateral dike formation process. Figure 15 illustrates such an intrusion sequence.

THE GLOBAL ROLE

Like a staircase to the mid-Atlantic ridge, Iceland's Reykjanes ridge descends to become one element of the planet's largest magmatic system and principal volcanic feature: the active centers of sea floor spreading. It is natural, then, to wonder if the relations we have discovered for Hawaii and Iceland have counterparts within these larger rift zones that form the active constructional plate margins (Figure 16). Firm constraints of the kind obtained at Mauna Loa, Kilauea and Krafla are not available and must await the development of spreading center observatories. As a working hypothesis, however, it is suggested that spreading center magma reservoirs and rift systems have a relative depth extent for shallow magmatic storage comparable to that of Iceland, that they are characterized by a pervasive region of neutral buoyancy beneath the median (axial) valley, and that this neutral buoyancy horizon regulates the manner in which magma is stored at shallow depths and is subsequently injected in oceanic rift systems. If such a hypothesis is correct, the existence of neutral buoyancy must have had a profound role in the mechanics and kine-

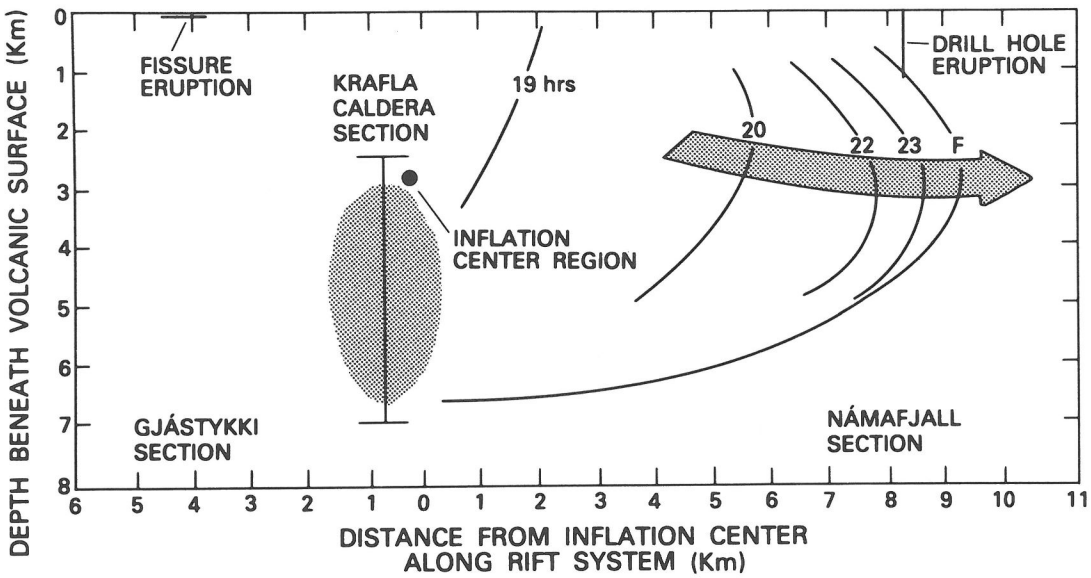

FIG. 15. Cross sectional profiles of the sequential position of the magmatic fracture front during rift zone intrusion from the Krafla central volcano, northeast Iceland. Numbers on the profiles are the times (in hours) following the onset of the intrusive phase. 'F' denotes the final position of the magmatic fracture front. The large shaded arrow delimits the time-depth-distance pathway followed by the parabolic apex of the intrusion as it moved along the inferred horizon of neutral buoyancy. The vertical bar that penetrates the aseismic region (shaded) beneath the Krafla caldera, delimits the maximum depth range of subcaldera magma storage. Parabolic intrusion profiles have been inferred by the progression of seismic hypocenter shifts within the rift zone. The inflation center is in essential coincidence with the inferred point of neutral buoyancy. The intrusion sequence culminated in a geothermal borehole eruption on 8 September 1977. Modified from BRANDSDÓTTIR and EINARSSON (1979).

matics of the plate accretionary process, as well as the manner in which shallow magmatic evolution has occurred as our planet has cooled and differentiated. We now marshall evidence supporting this hypothesis.

Direct observations by submersibles, and indirect photo reconnaissance by towed camera sleds, have revealed that the first order structural features of oceanic rift zone axial valley floors bear a striking resemblance to the eruptive and tectonic structures of subaerial basaltic rift zones. These features include:

(a) axial graben characteristically bounded by normal faulting (*e.g.*, HEKINIAN *et al.*, 1985);

(b) normal fault escarpments arranged in a terrace or staircase fashion away from the axial rift;

(c) shear normal fault escarpments of near vertical orientation that marginally bound flat valley floor blocks (*e.g.*, W. F. B. RYAN, 1985);

(d) dilatant fractures with crack-opening-displacements in the range 0.5 to 15 m (*e.g.*, HEKINIAN *et al.*, 1985; THOMPSON *et al.*, 1985);

(e) lava drainback structures attesting to large dilatant fracture volumes at depth, and drainback "bathtub rings", that record the incremental crack dilatations at depth which episodically lower the level of ponded lava lakes (*e.g.*, BALLARD *et al.*, 1979; RENARD *et al.*, 1985).

(f) hydrothermal venting associated with dilatant fracture networks (*e.g.*, RENARD *et al.*, 1985);

(g) gabbroic dike-like intrusives and dike "walls" exposed in three dimensions and in cross-section (*e.g.*, HEKINIAN *et al.*, 1985; HEY *et al.*, 1985);

(h) thin, sheeted basalt flows (*e.g.*, BALLARD *et al.*, 1979); and

(i) the common development of en echelon fractures throughout the valley floor. These may be eruptive or non-eruptive (*e.g.*, HEKINIAN *et al.*, 1985).

The continued imprint of these surface structures may be seen in cross-sectional seismic velocity profiles taken by refraction surveys across and along oceanic rift systems. Two surveys of the East Pacific Rise illustrate this structure. REID *et al.* (1977) conducted a seismic refraction survey at 21°N latitude on a central portion of the rise segment bounded

Table 1. Approximate lithologic and density relationships in the Icelandic crust

Layer number				Density
depth thickness (m)		Refs.	Geologic environment	ρ (g/cm^3)
0–1000	0	[1] [2] [3] [4] [5]	Relatively fresh and heavily fractured basalt of the surficial layer containing dilatant fractures. Hyaloclastic tuffs and breccias. Thickness: 0–1 km within the active volcanic zones.	2.1–2.5
T: 500–2000 m; average $T \approx 1000$ m	1	[1] [2] [5]	The Tertiary and Quaternary basaltic sequence. Progressively altered with increasing depth. On either side of the active volcanic zones. Beneath layer of minor intercalated tuff layers in the neovolcanic zones.	2.60
T: 1000–3000 m aver. $T \approx 2100$ m	2	[1] [2] [5]	Flood basalts locally intruded with basic and acidic rock masses.	2.65
$T \approx 4000$–5000 m	3	[1] [2] [5]	Basaltic. Equivalent to the oceanic layer. Heavily intruded with gabbroic dikes. Increasingly metamorphosed. Locally elevated beneath central volcanoes.	2.9
	4		Upper Mantle	3.1

[1] PÁLMASON (1963).
[2] PÁLMASON (1971).
[3] BJÖRNSSON *et al.* (1972).
[4] TÓMASSON and KRISTMANNSDÓTTIR (1972).
[5] PÁLMASON and SAEMUNDSSON (1974).

by the Tamayo Fracture Zone to the north and the Rivera Fracture Zone to the south. The fractured and porous upper levels were characterized by a compressional wave gradient of $\approx$1.6 km/sec at the sea floor to $\approx$6.7 km/sec at a depth of 2.5 km. From 2.5 to 4.5 km, the low velocity of 4.6 to 4.7 km/sec suggested the presence of partial melt (a completely molten tholeiitic region is characterized by $V_p \approx 2.6$ km/sec). Beneath 4.5 km, V_p increased again to 6.5 km/sec, and then to 7.8 km/sec by a depth of 10 km. It is noteworthy that the interval 2 to 4.5 km brackets the region of neutral buoyancy inferred for the East Pacific Rise from *in-situ* density-velocity estimates, with allowance for the superjacent water column load. ORCUTT *et al.* (1976) conducted a refraction survey along the axis of the East Pacific Rise near the Siqueiros Fracture Zone. Near the rise crest, a low velocity zone was deduced over the depth interval 2.0 to 3.4 km, where $V_p \approx 4.8$ km/sec. The roof of the low velocity zone (LVZ) is characterized by a gradient from $\approx$5 km/sec near the sea floor, to 6.7 km/sec at 2 km. Beneath the LVZ is a gradient from 6.2 km/sec (at 3.4 km), to 7.7 km/sec at a depth of 6 km. As at 21°N, the interval 2 to 3.4 km embraces the estimated position of the horizon of neutral buoyancy. The low velocity zone inferred by ORCUTT *et al.* (1976) is completely confined to a position within the 10 km-wide central rise axis. Thus, at two relatively fast-spreading ridge segments, evidence in the form of a low velocity zone centered near 3 km depth suggests the presence of magma, and this is, in turn, consistent with the inferred position of the horizon of neutral buoyancy. For the relatively slow-spreading mid-Atlantic ridge segments, however, seismic refraction surveys have not produced clear evidence for magmatic storage. For example, the 3-component instrument surveys of FOWLER and MATTHEWS (1974) and FOWLER (1976, 1978) at the FAMOUS site (37°N latitude) as well as 45°N latitude, have demonstrated that no special attenuation was produced in shear waves beneath the axial valley.

How does neutral buoyancy work within the context of ridge crest volcanism and the tectonics of plate separation? Rising magma, driven by positive buoyancy, is stabilized at shallow depths (2–4 km) beneath the median valley of an active ridge. With respect to the valley axis along the segment strike, this is expected to be centrally located. The surface expression of the central magma reservoir beneath may include (a) a topographic high, (b) a horst, (c) well-developed hydrothermal venting, or (d) major collapse structures that are sub-circular in plan. Within the core of the reservoir will be the point of neutral buoyancy. During replenishment, rising parcels of melt may intertially overshoot this


9/4
10
3
1
5
6
4
19
2

point of neutral buoyancy, and be subsequently driven down by negative buoyancy forces, spreading outward and approaching the horizon of neutral buoyancy. The continued influx of magma raises the fluid pressure level to the *in-situ* tensile strength of the reservoir ceiling and walls. For regions mantling the reservoir, fluid pressures above lithostatic will lead to sill inflation above the complex, and the topographic highs developed on the surface of the mid–ocean ridge—as well as occasional central horsts—may be accentuated by these integrated episodes of sill emplacement.

Rupture of the reservoir walls is expected to occur preferentially along the strike of the median valley axis and at a depth of 2 to 3 km beneath the valley floor. This rupture will be close to or essentially coincident with the intersection of the horizon of neutral buoyancy and the reservoir wall. For the East Pacific Rise, the work of ORCUTT *et al.* (1976), suggests a depth of $\approx$3 km. *During rupture, magmatic injection occurs laterally. That is, the newly forming dike has a distinct upper and lower edge (keel), advances with a parabolic snout, and is connected to the central reservoir only at its rear. The lateral dike-forming injection process is controlled by the horizon of neutral buoyancy.* This is control achieved through a rough, integrated balance of positive and negative buoyancy forces as the injection event proceeds: magma at the top of the dike is driven down by the low density heavily fractured countryrock above, whereas magma along the keel of the dike is prevented from descending (or may be driven up) by the relatively high *in-situ* densities associated with the gabbroic and ultramafic lithologies beneath. The result is one of lateral dike emplacement with a median height coincident with a subhorizontal plane of neutral buoyancy (RYAN, 1987). Dike widths will be controlled by the elastic strain energy stored in the host rock at the moment of intrusion, a quantity proportional to the magnitude of the minimum compressive stress (σ_3) and the host rock elastic moduli (K, μ, E, ν). Injection will continue until overpressures within the magma chamber are reduced.

A point to be emphasized is the inherent efficiency in the lateral dike formation process—a direct result of the neutral buoyancy principle. Because of the negative and positive buoyancy forces along the top and the bottom of the dike, respectively, the lateral injection process is self–regulating. An approximately constant dike thickness means that for a given volume of magma released from the reservoir, dike height is conserved, because both the top and the bottom of the intrusion attempt to reach the horizon of neutral buoyancy. The result is the attainment of remarkable dike lengths over short time periods. In this manner, a centrally located magma reservoir can activate very long segments in the rise of a mid–ocean rift system. Hence the role of neutral buoyancy in the genesis and tectonics of oceanic crust plays a dual role: a mechanical rationale for the geometry and dynamics of dike formation within spreading centers, and a means of maximizing the efficiency of the lateral injection process along the rift zone axis—providing the hydraulic force required for lithospheric plate separation beneath the median axial valley. This conclusion is broadly consistent with the three–dimensional framework for oceanic ridge segments suggested by WHITEHEAD *et al.* (1984), and SCHOUTEN *et al.* (1985). It goes beyond it, however, in providing a mechanical rationale for the stability and dynamics of the mid-segment magma reservoirs and their associated rift zone intrusive complexes.

Figure 17 illustrates the role of the horizon of neutral buoyancy within the context of an oceanic spreading center. Magma produced during the ascent of an upper mantle diapir, collects within a central region of neutral buoyancy. Lateral injection along the horizon of neutral buoyancy occurs periodically, dissipating the fluid pressure within the reservoir and leading to dike formation episodes. This produces the endogenous growth and stretching of the newly-formed oceanic crust, and the development of axial graben.

THE MAGMATIC ENVIRONMENTS OF SUBDUCTION AND THE CONTINENTAL INTERIOR

As a series of concluding observations, the depth extents of subcaldera magma storage have been compiled from an extended range of volcanic cen-

FIG. 16. Generalized map of the world's ocean floor, showing the principal features of the active oceanic ridges, plate margins, and loci of oceanic rift zones and dike intrusion. Regions whose evolution is influenced by the neutral buoyancy principle are: (1) Hawaii; (2) Iceland; (3) East Pacific Rise; (4) Crater Lake; and (5) Rabaul Caldera, Papua, New Guinea. Additional centers hypothesized to have high-level magmatic storage and/or intrusion influenced by neutral buoyancy are the Earth's oceanic rift systems; (6) Usu Volcano, Hokkaido, Japan; (7) Phlegraean Fields, Italy; (8) Mt. Etna, Sicily; (9) Mt. St. Helens, Washington; and (10) Long Valley, California. Map modified from the Mercator projection of HEEZEN and THARP (1977).

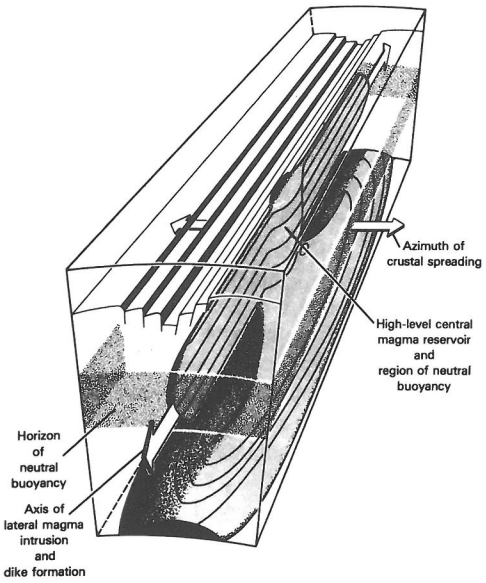

FIG. 17. Prismatic volume element of a spreading center ridge axis, illustrating the role of the horizon of neutral buoyancy (stippled horizon) in the origin and development of oceanic crust. The laterally-injected snouts of the magmatic fracture front, emanate from the central region of neutral buoyancy and move towards the front and rear of the reference volume. Mean sea level corresponds to the upper surface of the volume.

ters where geodetic and seismic monitoring have provided constraints. These include island arc, continental margin and continental interior settings, as well as inter-plate and intra-plate oceanic volcanoes. Figure 18 summarizes this depth distribution, and suggests the interval 1.5 to 5 km as a range that includes the depth region of inferred stored magma in 20 of the 21 plotted ranges. An exception occurs at Sakurajima Volcano, Japan, where an early analysis (MOGI, 1958), suggested a depth of 9–10 km.

Taken collectively, these observations embrace a wide spectrum of magma types, countryrock lithologies, and regional to local tectonic settings. To evaluate critically the proposition that these depth ranges represent the shallow equilibrium position of magma as influenced by neutral buoyancy, we require data on the *in-situ* density of the relevant magma types, as well as the vertical density profile appropriate to the countryrock of the volcanic edifices and their crustal foundations. Complete data sets of the type desired are not presently available for each of the centers listed in Figure 18; however, initial estimates at select centers may be made.

Modeling of the residual Bouguer gravity profiles for Cascade Range volcanoes has been undertaken by WILLIAMS and FINN (1986). After corrections for terraine effects, two- and three-dimensional modeling (CADY and SWEENEY, 1980; CORDELL and HENDERSON, 1968) of the Bouguer profiles produced by embedded polygons of variable density, have allowed inferences to be drawn about the sub-volcanic density distributions in cross-section. At Medicine Lake, Crater Lake, Newberry, Mount Hood, Mount Shasta and Mount St. Helens, the inferred densities of the volcanic edifices span the range 2.1–2.3 g/cm^3. For Mount St. Helens, this is compatible with the edifice density of 2.3 g/cm^3 used by JACHENS *et al.* (1981) in an interpretation of gravity changes during March–May, 1980.

High pressure falling-sphere densitometry experiments for Crater Lake andesite (KUSHIRO, 1978) have indicated densities of 2.57 ± 0.03 g/cm^3 at 1000 MPa and 1175°C, and 2.69 ± 0.03 g/cm^3 at 1250 MPa and 1200°C. For the low confining pressures appropriate to the near surface, the melt density (at 2.86 to 2.98 weight percent H_2O) may be expected to be somewhat less than Kushiro's (1978) measurement of 2.47 g/cm^3, evaluated at 500 MPa. Thus, on the basis of these observations, combined with the *in-situ* aggregate density of the volcanic edifice, Cascade magma may be expected to achieve mechanical equilibrium with its surroundings at shallow levels within and beneath the volcanic centers. Such an inference is then consistent with the concept of a horizon of neutral buoyancy beneath the Cascade system.

Additional evidence comes from Papua, New Guinea, and the recent unrest at Rabaul Caldera. Gravimetric monitoring of the caldera uplift associated with the intra-caldera seismicity of 1983–1984, has been conducted by MCKEE *et al.* (1984), who have observed (p. 406–407):

> "These (gravimetric) changes can be fully explained by the measured uplift if a density of about 1.9 g/cm^3 is assumed in the . . . near surface lithology within the caldera. The apparent absence of a gravity anomaly associated with the inferred magma body beneath the entrance to Great Harbour is possible due to lack of density contrast between the intruded magma and its surroundings. This suggests that the combined effects of hydrostatic head and buoyancy have allowed the magma to rise to a level at which its density matches its surroundings. At the estimated depth of the magma body (about 2 km), a density of 2.5 g/cm^3 can be derived . . . for the crustal rocks from their seismic velocity of about 4.5 km/sec. This value of density would be appropriate for a hydrous intermediate magma."

Thus, a synthesis of available data supports the hypothesis that the equilibrium resting place for the upper regions of subcaldera magma storage is coincident with the region of neutral buoyancy for the respective volcanic center.

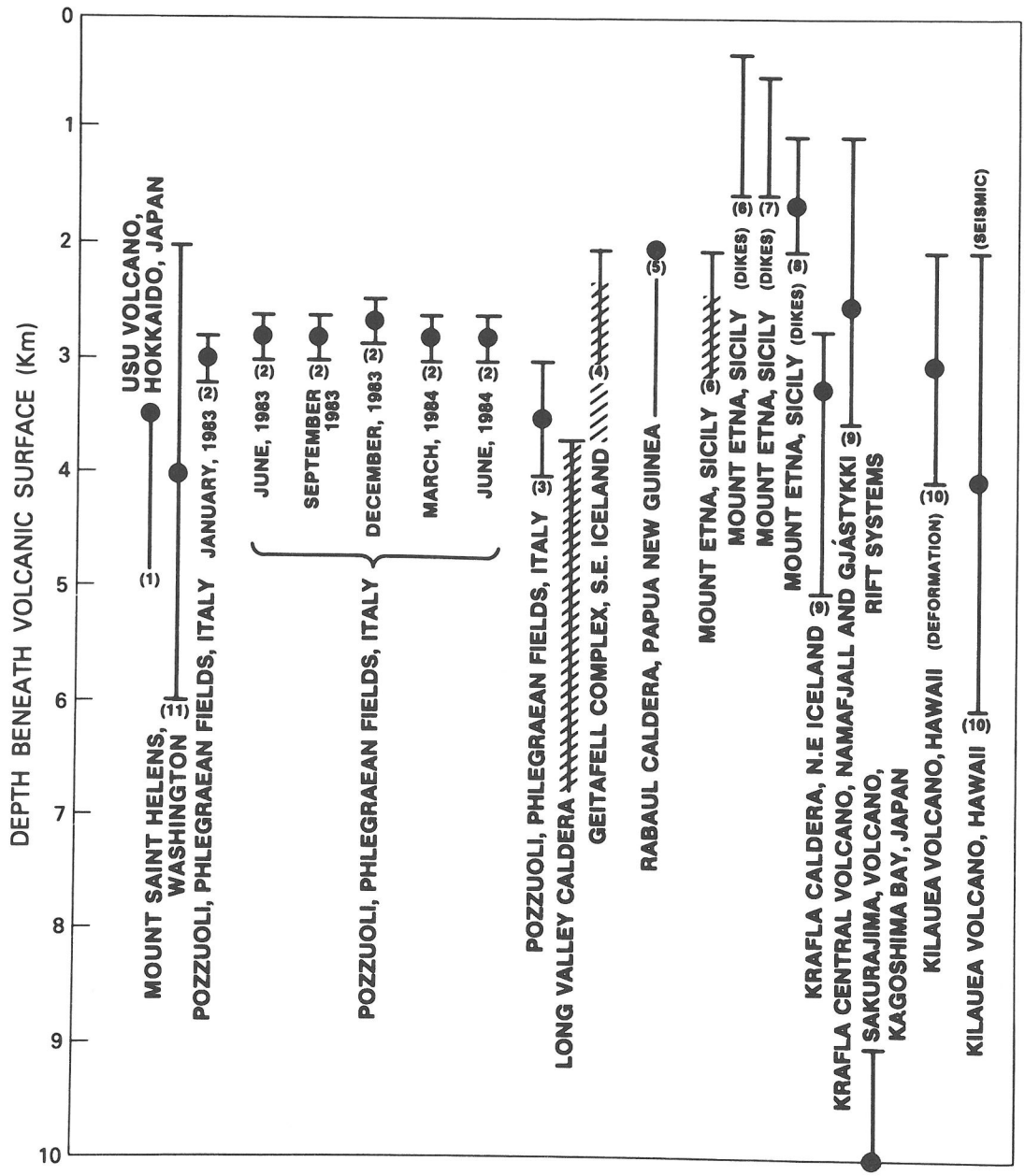

FIG. 18. The depth ranges for shallow magmatic storage in island arc, continental interior, interplate and intraplate oceanic settings. The compositional range spans the interval olivine tholeiite to rhyolite. Data sources for the respective magmatic centers are: (1) Usu volcano, Hokkaido, Japan; YOKOYAMA (1985). (2 and 3) Pozzuoli, Phlegraean fields, Italy, BERRINO *et al.* (1984), and ORTIZ *et al.* (1984); (4) Geitafell complex, southeast Iceland, FRIDLEIFSSON (1983); (5) Rabaul Caldera, Papua New Guinea, MCKEE *et al.* (1984); (6, 7 and 8) Mount Etna, Sicily, SANDERSON *et al.* (1983), SANDERSON (1982), MURRAY and GUEST (1982); (9a) Krafla Caldera, northeast Iceland, this report, Figure 13 and references therein; (9b) Krafla central volcano, Námafjall and Gjástykki rift systems, this report, Figure 14 and references therein; (10a) Kilauea volcano, Hawaii—deformation-based studies, this report, Figure 6a, and references therein; (10b) Kilauea volcano, Hawaii—seismic studies, this report, Figure 6a and references therein; (11) Mount Saint Helens, Washington, ENDO *et al.* (1981); (12) Sakurajima volcano, Kagoshima Bay, Japan; MOGI (1958). Long Valley, California, ELBRING and RUNDLE (1987), HILL (1976), HILL *et al.* (1985), KISSLING *et al.* (1984), MURPHY *et al.* (1985), RUNDLE *et al.* (1986), RYALL and RYALL (1981), SANDERS (1983, 1984), and STEEPLES and IYER (1976).

Volcanic eruptions within a neutral buoyancy context require episodes of continued volumetric displacement by new magma batches, high velocity inertial overshooting of the horizon of neutral buoyancy, the onset of differential vesiculation, or shallow and abrupt tectonic kneading. It is likely that many eruptions involve a subtle interplay of each of these factors. In a related consideration, high-momentum alkalic and kimberlitic fluids would be expected to experience significant decelleration in regions where their bulk density matched that of their surroundings.

SUMMARY RELATIONSHIPS

The three principal aspects of shallow magma reservoirs and their rift systems may be understood and integrated within the neutral buoyancy hypothesis.

(1) *Existence.* Beneath the heavily fractured veneer of active basaltic volcanoes, a crossover is produced between the *in-situ* densities of the edifice and tholeiitic melt. In Hawaii, the crossover occurs throughout the 2–7 km depth range, with the upper sections of this interval ($\approx$2 to $\approx$4 km) representing a region of inferred neutral buoyancy. The horizon of neutral buoyancy lies at $\approx$3 km local depth. For Kilauea and Mauna Loa, the region of neutral buoyancy has a 1:1 coincidence with the geodetically and seismically determined subcaldera magma reservoirs. Beneath the region, magma ascends under the influence of positive buoyancy forces, whereas above it, magma may descend by negative buoyancy. Within this region, magma is in approximate mechanical equilibrium with its surroundings. Thus, the neutral buoyancy of tholeiitic melt provides for the long–term stability and existence of magma reservoirs and their rift systems.

Intercomparisons between the depths of shallow emplacement and the *in-situ* density of their surroundings, suggests that the equilibrium position for the upper levels of magma in dioritic-andesitic centers and in granitic–rhyolitic complexes is also influenced by the neutral buoyancy principle.

(2) *Structure and function.* A 1:1 correspondence exists between the total depth range inferred for subcaldera magma storage and the depth extent required to eliminate fluid-accessible pore space in the absence of an applied pore pressure. In Hawaii, this characterizes Kilauea and Mauna Loa volcanoes, and in Iceland, it describes the Námafjall-Krafla–Gjástykki central volcano and rift systems.

The contractancy transition zone separates the shallow field of fracture and pore fluid compression from the deeper field of mineral compression, and corresponds to a depth equivalent of $\approx$200–300 MPa. This zone is coincident with the root section of magma reservoirs and the deepest keels of the active rift zone dike complexes. This general relationship also characterizes Kilauea, Mauna Loa, and Krafla.

For both Hawaiian and Icelandic rift systems, the lateral dike injection process follows the horizon of neutral buoyancy, where $\rho_{\text{countryrock}} \approx \rho_{\text{melt}}$, with the leading edge of dike advance tracking this horizon. Neutral buoyancy thus stabilizes dikes within their rifts, such that dike keels experience $\rho_{\text{countryrock}} - \rho_{\text{melt}} > 0$ (positive buoyancy), whereas dike tops are described by $\rho_{\text{countryrock}} - \rho_{\text{melt}} < 0$ (negative buoyancy). Therefore, the density contrasts associated with the Earth's near-surface produce a mechanism of "self regulation" in the dike injection process. It is Nature's way of maximizing dike lengths (per fixed magma volume) by minimizing dike height. It is this self–regulation that permits these intrusions to achieve such remarkable lengths in both Hawaiian and Icelandic rift systems. In a geometric context, the neutral buoyancy horizon regulates the dike height, the stored elastic strain energy in the surrounding countryrock regulates dike widths, and the available volume of stored magma within the reservoir regulates the total length of the newly formed dike. Rock contractancy produces the horizon of neutral buoyancy that orders this self–regulation process, and controls the details of the three–dimensional topography of neutral buoyancy regions at depth. The core of the region of neutral buoyancy is expected to be the favored locus of reservoir magma mixing, as well as the preferred depth for leakage into laterally-extensive rift systems.

(3) *Evolution.* As Hawaiian volcanoes increase in elevation and mature, their subcaldera reservoirs and acitve rifts undergo a progressive and systematic increase in elevation. This describes the progression from submarine infancy (*e.g.,* Loihi) to subaerial maturity (*e.g.,* Mauna Loa). The mechanical hallmarks of this evolutionary track involve the systematic and simultaneous elevation of the low density fractured veneer, the horizon of neutral buoyancy and the deeper transition region that separates the field of fracture and pore fluid compression (above 9 km local depth) from the field of mineral compression (below 10-km). In the wake of these rising reservoirs lie the older abandoned subsolidus reservoirs whose cores are characterized by high elastic wave velocities.

Within the oceanic crust, the process of lateral magma injection along the axis of rift segments, is expected to follow the horizon of neutral buoyancy.

A corollary of the neutral buoyancy-self regulation principle, is that the magma injection-dike formation contribution to plate separation is maximized along the segment strike—a consequence of the volume efficient magma partitioning process.

Thus constructed, the neutral buoyancy hypothesis brings new unity and order to a wide range of experimental, theoretical and observational data. It integrates the existence, the three-dimensional structure, the large and small-scale material properties, the short-term dynamics and the long-term evolutionary behavior of shallow portions of magmatic systems. While generally accepted separately, they have heretofore remained unrelated and uncorrelated.

Acknowledgments—The Conference convenors and the Geophysical Laboratory of the Carnegie Institution of Washington provided the forum for presenting major portions of this work. Ruthie Robertson prepared the typescript. Reginald Okamura of the Hawaiian Volcano Observatory provided logistical support, as did Axel Björnsson of Orkustofnun (The National Energy Authority of Iceland) and the staff of Kröfluvirkjun. Logistical support, and field conferences with Kristján Saemundson, Hjörtur Tryggvason and Eysteinn Tryggvason were most helpful. Field conferences in eastern and southeastern Iceland with Gudmundur Ómar Fridleifsson, Helgi Torfason and Karl Grönvold were much appreciated. The Nordic Volcanological Institute and Gudmundur Sigvaldasson are thanked for their hospitality. David P. Hill and Richard S. Williams, Jr. reviewed an early version of the manuscript, and suggested several changes for its improvement. Additional review comments by Axel Björnsson, Olafur Flovenz, Claude T. Herzberg, Bjorn O. Mysen, Frank J. Spera and Edward W. Wolfe led to further improvements. Fred Klein and John Rundle kindly provided preprints of recent work. Figures were prepared with the assistance of Lendell Keaton, Marcia Prins and M. Sandra Nelson. Resources available to M. P. Ryan under a Grove Karl Gilbert Fellowship of the Geologic Division of the U.S. Geological Survey provided partial support. Additional support was provided by the U.S. Dept. of Energy, under Interagency Agreement No. DE-AI01-86CE31002.

REFERENCES

BABUSKA V. (1972) Elasticity and anisotropy of dunite and bronzitite. *J. Geophys. Res.* **77,** 6955–6965.

BAJUK E. I., VALAROVICH M. P., KLIMA K., PROS Z. and VANEK J. (1957) Velocity of longitudinal waves in eclogite and ultrabasic rocks under pressures to 4 kilobars. *Stud. in Geophys. and Geod.* **11,** 271.

BALLARD R. D., HOLCOMB R. T. and VAN ANDEL TJ. H. (1979) The Galapagos Rift at 86°W; 3. Sheet flows, collapse pits, and lava lakes of the rift valley. *J. Geophys. Res.* **84,** 5407–5422.

BENDER J. F., HODGES F. N. and BENCE A. E. (1978) Petrogenesis of basalts from the project FAMOUS area: experimental study from 0 to 15 Kbars. *Earth Planet. Sci. Lett.* **41,** 277–302.

BERRINO G., CORRADO G., LUONGO G. and TORO B. (1984) Ground deformation and gravity changes accompanying the 1982 Pozzuoli uplift. *Bull. Volcanol.* **47-2,** 187–200.

BIRCH F. (1960) Velocity of compressional waves in rocks to 10 kilobars, Part I. *J. Geophys. Res.* **65,** 1083–1102.

BJÖRNSSON A. (1985) Dynamics of crustal rifting in NE Iceland. *J. Geophys. Res.* **90,** 10,151–10,162.

BJÖRNSSON A. and SIGURDSSON O. (1978) Hraungos úr borholu i Bjarnarflagi. *Náttúru Fraedingurinn,* 19–23.

BJÖRNSSON S., ANÓRSSON S. and TÓMASSON J. (1972) Economic evaluation of the Reykjanes thermal brine area. *Geothermics,* **2,** Special issue 2, 1640–1650.

BJÖRNSSON A., JOHNSEN G., SIGURDSSON S., THORBERGSSON G. and TRYGGVASON E. (1979) Rifting of the plate boundary in north Iceland 1975–1978. *J. Geophys. Res.* **84,** 3029–3038.

BODVARSSON G. and WALKER G. P. L. (1964) Crustal drift in Iceland. *Geophys. J. Roy. Astron. Soc.* **8,** 285–300.

BRACE W. F. (1971a) Resistivity of saturated crustal rocks to 40 km. based on laboratory measurements. In *The Structure and Properties of the Earth's Crust,* American Geophysical Union Monograph 14, pp. 243–255.

BRACE W. F. (1971b) Micromechanics in rock systems. In *Solid Mechanics and Engineering Design,* (ed. M. TE'ENI), PART I, pp. 1878–2004. John Wiley–Interscience, London.

BRACE W. F. (1972) Pore pressure in geophysics. In *Flow and Fracture of Rocks,* Geophys. Monograph, Vol. 16, pp. 265–274 John Wiley.

BRACE W. F. and ORANGE A. S. (1968a) Electrical resistivity changes in saturated rocks during fracture and frictional sliding. *J. Geophys. Res.* **73,** 1433–1445.

BRACE W. F. and ORANGE A. S. (1968b) Further studies of the effect of pressure on electrical resistivity of rocks. *J. Geophys. Res.* **73,** 5407–5420.

BYERLEE J. D. (1968) The brittle-ductile transition in rocks. *J. Geophys. Res.* **73,** 4741–4750.

BRANDSDÓTTIR B. and EINARSSON P. (1979) Seismic activity associated with the September 1977 deflation of the Krafla central volcano in northeastern Iceland. *J. Volcanol. Geothermal. Res.* **6,** 197–212.

CADY J. W. and SWEENEY R. E. (1980) Program ZHDPOT for 2½ dimensional gravity and magnetic modeling: SEG suppl. to CADY, J. W., Calculation of gravity and magnetic anomalies of finite length right rectangular prisms. *Geophysics* **45,** 1507–1512.

CHASE T., MILLER C. P., SEEKINS B. A., NORMARK W. R., GUTMACHER C. E., WILDE P. and YOUNG J. D. (1980) Topography of the Southern Hawaiian Islands. *U.S. Geol. Survey Open File Map 81-120.*

CHRISTENSEN N. I. (1966) Elasticity of ultrabasic rocks. *J. Geophys. Res.* **71,** 5921–5931.

CHRISTENSEN N. I. (1971) Fabric, seismic anisotropy and tectonic history of the Twin Sisters dunite. *Bull. Geol. Soc. Amer.* **82,** 1681–1694.

CHRISTENSEN N. I. (1973) Compressional and shear wave velocities in basaltic rocks, DSDP leg 16. In *Initial Reports of the Deep Sea Drilling Project,* (eds. T. H. VAN ANDEL, G. R. HEATH and others), Vol. 16, pp. 647 U.S. Government Printing Office.

CHRISTENSEN N. I. (1974) The petrologic nature of the lower oceanic crust and upper mantle. In *Geodynamics of Iceland and the North Atlantic Area,* (ed. KRISTJANSSON), pp. 165–176 D. Reidel Publ. Co. Dordrecht, Netherlands.

CHRISTENSEN N. I. (1976) Seismic velocities, densities and

elastic constants of basalts from DSDP leg 35. In *Initial Reports of the Deep Sea Drilling Project,* (eds. C. D. HOLLISTER, C. CRADDOCK *et al.*), Vol. 35, pp. 335–337 U.S. Government Printing Office.

CHRISTENSEN N. I. (1978) Ophiolites, seismic velocities and oceanic crustal structure. *Tectonophys.* **47,** 131–157.

CHRISTENSEN N. I. and RAMANANANTOANDRO R. (1971) Elastic moduli and anisotropy of dunite to 10 kilobars. *J. Geophys. Res.* **76,** 4003–4010.

CHRISTENSEN N. I. and SALISBURY M. H. (1972) Sea floor spreading, progressive alteration of layer two basalts, and associated changes in seismic velocities. *Earth Planet. Sci. Lett.* **15,** 367–375.

CHRISTENSEN N. I. and SALISBURY M. H. (1973) Velocities, elastic moduli and weathering-age relations for Pacific layer 2 basalts. *Earth Planet. Sci. Lett.* **19,** 461–470.

CHRISTENSEN N. I. and SALISBURY M. H. (1975) Structure and constitution of the lower oceanic crust. *Rev. of Geophysics Space Physics* **13,** 57–86.

CHRISTENSEN N. I. and WILKENS R. H. (1982) Seismic properties, density, and composition of the Icelandic crust near Reydarfjördur. *J. Geophys. Res.* **87,** 6389–6395.

CHRISTENSEN N. I., CARLSON R. L., SALISBURY M. H. and FOUNTAIN D. M. (1974a) Velocities and elastic moduli of volcanic and sedimentary rocks recovered on DSDP leg 25. In *Initial Reports of the Deep Sea Drilling Project,* (eds. E. S. W. SIMPSON, R. SCHLICH *et al.*), Vol. 25, pp. 357–360 U.S. Government Printing Office.

CHRISTENSEN N. I., SALISBURY M. H., FOUNTAIN D. M. and CARLSON R. L. (1974b) Velocities of compressional and shear waves in DSDP leg 27 basalts. In *Initial Reports of the Deep Sea Drilling Project,* (eds. J. J. VEEVERS and J. R. HEIRTZLER), Vol. 27, pp. 445–449 U.S. Government Printing Office.

CHRISTENSEN N. I., CARLSON R. L., SALISBURY M. H. and FOUNTAIN D. M. (1975) Elastic wave velocities in volcanic and plutonic rocks recovered on DSDP leg 31. In *Initial Reports of the Deep Sea Drilling Project,* (eds. D. E. KRAIG, J. C. INGLE *et al.*), Vol. 31, pp. 607–609 U.S. Government Printing Office.

CORDELL L. and HENDERSON R. (1968) Iterative three-dimensional solution of gravity data using a digital computer. *Geophysics* **33,** 596–601.

CROSSON R. S. and KOYANAGI R. Y. (1979) Seismic velocity structure below the island of Hawaii from local earthquake data. *J. Geophys. Res.* **84,** 2331–2342.

DAVIS P. M., HASTIE L. M. and STACEY F. D. (1974) Stresses within an active volcano—with particular reference to Kilauea. *Tectonophys.* **22,** 355–362.

DAVIS P. M. (1986) Surface deformation due to inflation of an arbitrarily oriented triaxial ellipsoidal cavity in an elastic half-space, with reference to Kilauea Volcano, Hawaii. *J. Geophys. Res.* **91,** 7429–7438.

DECKER R. W., KOYANAGI R. Y., DVORAK J. J., LOCKWOOD, J. P., OKAMURA A. T., YAMASHITA K. M. and TANIGAWA W. R. (1983) Seismicity and surface deformation of Mauna Loa volcano, Hawaii. *EOS* **64,** 545–547.

DIETERICH J. H. and DECKER R. W. (1975) Finite element modeling of surface deformation associated with volcanism. *J. Geophys. Res.* **80,** 4094–4102.

DUFFIELD W. A., CHRISTENSEN R. L., KOYANAGI R. Y. and PETERSON D. W. (1982) Storage, migration and eruption of magma at Kilauea volcano, Hawaii, 1971–1972. *J. Volcanol. Geothermal. Res.* **13,** 273–307.

DVORAK J., OKAMURA A. and DIETERICH J. H. (1983) Analysis of surface deformation data, Kilauea volcano, Hawaii: October 1966 to September 1970. *J. Geophys. Res.* **88,** 9295–9304.

EATON J. P. (1962) Crustal structure and volcanism in Hawaii. In *Crust of the Pacific Basin,* Amer. Geophys. Union Monograph 6, pp. 13–29.

EINARSSON P. (1978) S-wave shadows in the Krafla caldera in NE-Iceland, evidence for a magma chamber in the crust. *Bull. Volcanol.* **41–3,** 1–9.

EINARSSON P. and BRANDSDÓTTIR B. (1980) Seismological evidence for lateral magma intrusion during the July 1978 deflation of the Krafla volcano in NE-Iceland. *J. Geophys.* **47,** 160–165.

ELBRING G. J. and RUNDLE J. B. (1987) Analysis of borehole seismograms from Long Valley, California: implications for caldera structure. *J. Geophys. Res.* (In press)

ENDO E. T., MALONE S. D., NOSON L. L. and WEAVER S. C. (1981) Locations, magnitudes and statistics of the March 20–May 18 earthquake sequence. In The 1980 eruptions of Mount St. Helens, Washington (eds. P. W. LIPMAN and D. R. MULLINEAUX). *U.S. Geol. Surv. Prof. Paper 1250.*

FEDOTOV S. A. (1977) Mechanism of deep-seated magmatic activity below island-arc volcanoes and similar structures. *Int. Geol. Rev.* **19,** 671–680.

FISKE R. S. and KINOSHITA W. T. (1969) Inflation of Kilauea volcano prior to its 1967–1968 eruption. *Science* **165,** 341–349.

FLOVENZ O. G. (1980) Seismic structure of the Icelandic crust above layer three and the relation between body wave velocity and the alteration of the basaltic crust. *J. Geophys.* **47,** 211–220.

FLOVENZ O. G., GEORGSSON L. S. and ARNASON K. (1985) Resistivity structure of the upper crust in Iceland. *J. Geophys. Res.* **90,** 10,136–10,150.

FOX D. G. (1970) Forced plume in a stratified fluid. *J. of Geophys. Res.* **75,** 6818–6835.

FOX P. J. and SCHREIBER E. (1973) Compressional wave velocities in basalt and dolerite samples recovered during leg 15. In *Initial Reports of the Deep Sea Drilling Project,* (eds. N. T. EDGAR, J. B. SAUNDERS *et al.*), Vol. 15, pp. 1013–1016. U.S. Government Printing Office.

FOX P. J., SCHREIBER E. and PETERSON J. J. (1973) The geology of the Oceanic crust: Compressional wave velocities of oceanic rocks. *J. Geophys. Res.* **78,** 5155–5172.

FOWLER C. M. R. (1976) Crustal structure of the Mid-Atlantic ridge crest at 37°N. *Geophys. J. Roy. Astron. Soc.* **47,** 459–591.

FOWLER C. M. R. (1978) The Mid-Atlantic ridge: structure at 45°N. *Geophys. J. Roy. Astron. Soc.* **54,** 167–183.

FOWLER C. M. R. and MATTHEWS D. H. (1974) Seismic refraction experiment on the Mid-Atlantic Ridge in the FAMOUS area. *Nature* **249,** 752–754.

FRIDLEIFSSON G. O. (1983) The geology and the alteration history of the Geitafell central volcano, southeast Iceland. Ph.D. Thesis, Grant Institute of Geology, University of Edinburgh.

FUJII T. and KUSHIRO I. (1977) Density, viscosity, and compressibility of basaltic liquid at high pressures. *Carnegie Inst. Wash. Yearb.* **76,** 419–424.

GOODMAN R. E. (1976) Methods of geological engineering

in discontinuous rocks. 472 p. West Publishing Co. St. Paul.

GOODMAN R. E. and DUBOIS J. (1972) Duplication of dilatancy in analysis of jointed rocks. Jour. of the Soil Mechanics and Foundations Division, *Proceedings of the American Society of Civil Engineers 98,* 399–422.

GREENLAND L. P., ROSE W. I. and STOKES J. B. (1985) An estimate of gas emissions and magmatic gas content from Kilauea volcano. *Geochem. Cosmochim. Acta* **49,** 125–129.

HAWAII INSTITUTE OF GEOPHYSICS (1965) Data from gravity surveys over the Hawaiian archipelago and other Pacific islands. *Hawaii Inst. Geophys. Rept. 65-4.* 10 tables.

HEEZEN B. C. and THARP M. (1977) (Map of) the World's Ocean Floor. Mercator Projection. Scale: 1:23,230,300. United States Navy, Office of Naval Research.

HEKINIAN R., AUZENDE J. M., FRANCHETEAU J., GENTE P., RYAN W. B. F. and KAPPEL E. S. (1985) Offset spreading centers near 12°53′N on the east Pacific rise: submersible observations and composition of the volcanics. *Marine Geophys. Res.* **7,** 359–377.

HEY R., SINTON J. M., ATWATER T. M., CHRISTIE D. M., JOHNSON H. P., KLEINROCK M. C., MACDONALD K. C., MILLER S. P., NEAL C. A., SEARLE R. C., SLEEP N. H. and YONOVER R. N. (1985) Alvin investigation of an oceanic propagating rift system, Galapagos 95.5°W. *EOS* **66,** 1091.

HILL D. P. (1969) Crustal structure of the island of Hawaii from seismic–refraction measurements. *Bull. Seis. Soc. Amer.* **59,** 101–130.

HILL D. P. (1976) Structure of Long Valley caldera, California, from a seismic refraction experiment. *J. Geophys. Res.* **81,** 745–753.

HILL D. P., KISSLING E., LUETGERT J. H. and KRADOLFER V. (1985) Constraints on the upper crustal structure of Long Valley-Mono Craters volcanic complex of eastern California, from seismic refraction measurements. *J. Geophys. Res.* **90,** 11,135–11,150.

HIMASEKHAR K. and JALURIA Y. (1982) Laminar buoyancy-induced axisymmetric free boundary flows in a thermally stratified medium. *Int. J. Heat and Mass Transfer* **25,** 213–221.

HIRST E. (1971) Buoyant jets discharged to quiescent stratified ambients. *J. Geophys. Res.* **76,** 7375–7384.

HUGHES D. S. and CROSS J. H. (1951) Elastic wave velocities in rocks at high pressures and temperatures. *Geophysics* **16,** 577–593.

HUPPERT H. E. and SPARKS R. S. J. (1980) Restrictions on the compositions of mid–ocean ridge basalts: a fluid dynamical investigation. *Nature* **286,** 46–48.

HUPPERT H. E., SPARKS R. S. J., WHITEHEAD J. A. and HALLWORTH M. A. (1986) Replenishment of magma chambers by light inputs. *J. Geophys. Res.* **91,** 6113–6122.

HYNDMAN R. D. (1976) Seismic velocity measurements of basement rocks from DSDP leg 37. In *Initial Reports of the Deep Sea Drilling Project,* (eds. F. AUMENTO and W. G. MELSON), Vol. 37, pp. 373–387 U.S. Government Printing Office.

JACHENS R. C., SPYDELL R. D., PITTS G. S., DZURISIN D. and ROBERTS C. W. (1981) Temporal gravity variations at Mount St. Helens, March–May, 1980. In *The 1980 Eruptions of Mount St. Helens, Washington,* (eds. P. W. LIPMAN, D. R. MULLINEAUX). U.S. Geological Survey Professional Paper 1250, 193–200.

JACKSON D. B., SWANSON, D. A., KOYANAGI R. Y. and WRIGHT T. L. (1975) The August and October 1968 east rift eruptions of Kilauea volcano, Hawaii. *U.S. Geol. Surv. Prof. Paper 890,* 33 p.

JACKSON E. D. (1968) The character of the lower crust and upper mantle beneath the Hawaiian Islands. Prague, *XXIII International Geological Congress* **1,** 135–150.

JALURIA Y. (1986) Hydrodynamics of laminar buoyant jets. In *Encyclopedia of Fluid Mechanics,* Chap. 12, pp. 317–348 Gulf Publ. Co., Houston.

JOHNSON A. M. and POLLARD D. D. (1973) Mechanics of growth of some laccolithic intrusions in the Henry mountains, Utah, I. *Tectonophys.* **18,** 261–309.

JOHNSEN G. V., BJÖRNSSON A. and SIGURDSON S. (1980) Gravity and elevation changes caused by magma movement beneath the Krafla caldera, northeast Iceland. *J. Geophys. Res.* **47,** 132–140.

KANAMORI H. and MIZUTANI (1965) Ultrasonic measurements of elastic constants of rocks under high pressures. *Bull. Earthquake Res. Inst.* **43,** 173.

KING M. S. (1966) Wave velocities in rocks as a function of changes in overburden pressure and pore fluid saturants. *Geophysics* **31,** 50–73.

KINOSHITA W. T. (1965) A gravity survey of the island of Hawaii. *Pac. Sci.* **19,** 339–340.

KINOSHITA W. T. and OKAMURA R. T. (1965) A gravity survey of the island of Maui, Hawaii. *Pac. Sci.* **19,** 341–342.

KISSLING E., ELLSWORTH W. and COCKERHAM R. S. (1984) Three–dimensional structure of the Long Valley caldera, California, region by geotomography. *U.S. Geological Survey Open File Report 84-939,* 188–220.

KLEIN F. W. (1981) A linear gradient crustal model for south Hawaii. *Bull. Seis. Soc. Amer.* **71,** 1503–1510.

KLEIN F. W., KOYANAGI R. Y., NAKATA J. S. and TANIGAWA W. R. (1987) The seismicity of Kilauea's magma system. In *U.S. Geological Survey Professional Paper 1350,* (eds. R. W. DECKER, T. L. WRIGHT and P. H. STAUFFER). (In press).

KOYANAGI R. Y., UNGER J. D., ENDO E. T. and OKAMURA A. T. (1976) Shallow earthquakes associated with inflation episodes at the summit of Kilauea volcano, Hawaii. *Bull. Volcanol.* **39,** 621–631.

KROENKE L. W., MANGHNANI M. H., RAI C. S., FRYER P. and RAMANANANTOANDRO R. (1976) Elastic properties of selected ophiolitic rocks from Papua, New Guinea: nature and composition of oceanic crust and upper mantle. In *The Geophysics of the Pacific Ocean Basin and its Margins,* (eds. G. H. SUTTON, M. H. MANGHNANI and R. MOBERLY), American Geophysical Union Monograph 19, p. 407.

KUSHIRO I. (1978) Density and viscosity of hydrous calc-alkalic andesite magma at high pressures, *Carnegie Inst. Wash. Yearb.* **77,** 675–677.

LARSEN G., GRÖNVOLD K. and THORARINSSON S. (1979) Volcanic eruption through a geothermal borehole at Námafjall, Iceland. *Nature* **278,** 707–710.

MANGHNANI M. H. and WOOLLARD G. P. (1968) Elastic wave velocities in Hawaiian rocks at pressures to 10 kilobars. In *The Crust and Upper Mantle of the Pacific Area* (eds. L. KNOPOFF, C. L. DRAKE and P. J. HART), American Geophysical Union Monograph 12, pp. 501.

MAO N.-H., ITO J., HAYS J. F., DRAKE J. and BIRCH F. (1970) Composition and elastic constants of Hortonolite Dunite. *J. Geophys. Res.* **75,** 4071–4076.

MARQUART G. and JACOBY W. (1985) On the mechanism

of magma injection and plate divergency during the Krafla rifting episode in NE-Iceland. *J. Geophys. Res.* **90,** 10,178–10,192.

McBIRNEY A. R. and AOKI K. (1968) Petrology of the island of Tahiti. *Geol. Soc. Amer. Mem.* **116,** 523–556.

McKEE C. O., LOWENSTEIN P. L., DeSAINT OURS P., TALAI B., ITIKARI I. and MORI J. J. (1984) Seismic and ground deformation crises at Rabul Caldera: prelude to an eruption? *Bull. Volcanol.* **47-2,** 397–411.

MIZUTANI H. and NEWBIGGING D. F. (1973) Elastic wave velocities of Apollo 14, 15 and 16 rocks. *Proceedings of the Fourth Lunar Science Conference 4-3,* 2601.

MOGI K. (1958) Relations between the eruptions of various volcanoes and the deformations of the ground surfaces around them. *Bull. Earthquake Res. Inst.* **36,** 99–134. University of Tokyo.

MOORE J. G. (1965) Petrology of deep sea basalt near Hawaii. *Amer. J. Sci.* **263,** 40–52.

MURPHY W. J., RENAKER E., ROBERTSON M., MARTIN A. and MALIN P. E. (1985) The 1985 mammoth wide-angle reflection surey. *EOS* **66,** 960.

MURRAY J. B. and GUEST J. E. (1982) Vertical ground deformation on Mount Etna, 1975–1980. *Bull. Geol. Soc. Amer.* **93,** 1160–1175.

ORCUTT J. A., KENNETT B. L. N. and DORMAN L. M. (1976) Structure of the east Pacific rise from an ocean bottom seismometer survey. *Geophys. J. Roy. Astron. Soc.* **45,** 305–320.

ORTIZ R., ARAÑA V., ASTIZ M. and VALENTIN A. (1984) Magnetotelluric survey in the Bradyseismic area of Phlegraean Fields. *Bull. Volcanol.* **47-2,** 239–246.

PÁLMASON G. (1963) Seismic refraction investigation of the basalt lavas in northern and eastern Iceland. *Jökull* **3,** 40–60.

PÁLMASON G. (1971) Crustal structure of Iceland from explosion seismology. *Soc. Sci. Islandica,* **RIT XL.**

PÁLMASON G. and SAEMUNDSSON K. (1974) Iceland in relation to the mid-Atlantic ridge. *Ann. Rev. of Earth and Planetary Sci.* **2.**

POLLARD D. D., DELANEY P. T., DUFFIELD W. A., ENDO E. T. and OKAMURA A. T. (1983) Surface deformation in volcanic rift zones. *Tectonophys.* **94,** 541–584.

RAO M., RAMANA Y. V. and GOGTE B. S. (1974) Dependence of compressional velocity on the mineral chemistry of eclogites. *Earth Planet. Sci. Lett.* **23,** 15–20.

REID I., ORCUTT J. A. and PROTHERO W. A. (1977) Seismic evidence for a narrow zone of partial melting underlying the east Pacific rise at 21°N. *Bull. Geol. Soc. Amer.* **88,** 678–682.

RENARD V., HEKINIAN R., FRANCHETEAU J., BALLARD R. D. and BACKER H. (1985) Submersible observations at the axis of the ultra-fast-spreading east Pacific rise (17°30′ to 21°30′S). *Earth Planet. Sci. Lett.* **75,** 339–353.

RODI W. (ed.) (1982) *Turbulent Buoyant Jets and Plumes.* 184 p. Pergamon Press, Oxford.

RUNDLE J. B., CARRIGAN C. R., HARDEE H. C. and LUTH W. C. (1986) Deep drilling to the magmatic environment in Long Valley, California. *EOS* **67,** No. 21, 490–491.

RYALL F. and RYALL A. (1981) Attenuation of P and S waves in a magma chamber in Long Valley, California. *Geophys. Res. Lett.* **8,** 557.

RYAN M. P. (1985) The contractancy mechanics of magma reservoir and rift system evolution. *EOS* **66,** 854.

RYAN M. P. (1987) The elasticity and contractancy of Hawaiian olivine tholeiite, and its role in the stability and structural evolution of sub-caldera magma reservoirs and rift systems. In *U.S. Geological Survey Professional Paper 1350.* (eds. R. W. DECKER, T. L. WRIGHT and P. STAUFFER). (In Press).

RYAN M. P., KOYANAGI R. Y. and FISKE R. S. (1981) Modeling the three-dimensional structure of magma transport systems: application to Kilauea volcano, Hawaii. *J. Geophys. Res.* **86,** 7111–7129.

RYAN M. P., BLEVINS J. Y. K., OKAMURA A. T. and KOYANAGI R. Y. (1983) Magma reservoir subsidence mechanics: theoretical summary and application to Kilauea volcano, Hawaii. *J. Geophys. Res.* **88,** 4147–4181.

RYAN W. B. F. (1985) Back-spreading of the mid-ocean ridge axis using a model that incorporates features of shield volcanoes and seamounts. *EOS* **66,** 1091.

SALISBURY M. H. and CHRISTENSEN N. I. (1976) Sonic velocities and densities of basalts from the Nazca Plate, DSDP leg 34. In *Initial Reports of the Deep Sea Drilling Project* (eds. R. S. YEATS, S. R. HART *et al.*), Vol. 34, pp. 543–546 U.S. Government Printing Office.

SANDERS C. O. (1983) Location and configuration of magma bodies beneath Long Valley, California, determined from anamolous earthquake signals (abstr.). *EOS* **64,** (45), 890.

SANDERS C. O. (1984) Location and configuration of magma bodies beneath Long Valley, California, determined from anomalous earthquake signals. *J. Geophys. Res.* **89,** 8287–8302.

SANDERSON T. J. O. (1982) Direct gravimetric detection of magma movements at Mount Etna. *Nature* **297,** 487–490.

SANDERSON T. J. O., BERRINO G., CORVADO G. and GRIMALDI M. (1983) Ground deformation and gravity changes accompanying the March 1981 eruption of Mount Etna. *J. Volcanol. Geotherm. Res.* **16,** 299–315.

SCHOUTEN H., KLITGORD K. D. and WHITEHEAD J. A. (1985) Segmentation of mid-ocean ridges. *Nature* **317,** 225–229.

SCHREIBER E., FOX P. J. and PETERSON J. J. (1972) Compressional wave velocities in selected samples of gabbro, schist, limestone, anhydrogypsum and halite. In *Initial reports of the Deep Sea Drilling Project* (eds. W. B. F. RYAN, K. J. HSU *et al.*), Vol. 13, pp. 595–597 U.S. Government Printing Office.

SCHREIBER E., FOX P. J. and PETERSON J. J. (1974) Compressional wave velocities in samples recovered from DSDP leg 24. In *Initial reports of the Deep Sea Drilling Project,* (eds. R. L. FISHER *et al.*), Vol. 24, pp. 787–790 U.S. Government Printing Office.

SHIBATA T., DELONG S. E. and WALKER D. (1979) Abyssal tholeiites from the Oceanographer fracture zone. I. Petrology and fractionation. *Contrib. Mineral. Petrol.* **70,** 89–102.

SPARKS R. S. J. and HUPPERT H. E. (1984) Density changes during the fractional crystallization of basaltic magmas: fluid dynamic implications. *Contrib. Mineral. Petrol.* **85,** 300–309.

STEEPLES D. W. and IYER H. M. (1976) Low velocity zone under Long Valley as determined from teleseismic events. *J. Geophys. Res.* **81,** 849–860.

STOLPER E. and WALKER D. (1980) Melt density and the average composition of basalt. *Contrib. Mineral. Petrol.* **74,** 7–12.

SWANSON D. A., JACKSON D. B., KOYANAGI R. Y. and WRIGHT T. L. (1976) The February 1969 east rift eruption of Kilauea volcano, Hawaii. *U.S. Geological Survey Professional Paper 891,* 30 pp.

THOMPSON G., BRYAN W. B., BALLARD R., HAMURO K.

and MELSON W. G. (1985) Axial processes along a segment of the east Pacific rise, 10°–12°N. *Nature* **318,** 429–433.

TODD T. and SIMMONS G. (1972) Effect of pore pressure on the velocity of compressional waves in low-porosity rocks. *J. Geophys. Res.* **77,** 3731–3743.

TÓMASSON J. and KRISTMANNSDÓTTIR H. (1972) High temperature alteration minerals and thermal brines, Reykjanes, Iceland. *Contrib. Mineral. Petrol.* **36,** 123–134.

TRYGGVASON E. (1980) Observed ground deformation during the Krafla eruption of March 16, 1980. *Nordic Volcanol. Inst. Rept. 80-05,* 12 pp.

TRYGGVASON E. (1981) Pressure variations and volume of the Krafla magma reservoir. *Nordic Volcanol. Inst. Rept. 81-05,* University of Iceland, 17 pp.

TRYGGVASON E. (1984) Widening of the Krafla fissure swarm during the 1975–1981 volcano tectonic episode. *Bull. Volcanol.* **47-1,** 47–69.

TRYGGVASON E. (1986) Multiple magma reservoirs in a rift zone volcano: Ground deformation and magma transport during the September 1984 eruption of Krafla, Iceland. *J. Volcanol. Geotherm. Res.* **28,** 1–44.

WALKER G. P. L. (1959) Geology of the Reydarfjordur area, eastern Iceland. *Quart. J. Geol. Soc. London* **114,** 367–393.

WALKER G. P. L. (1963) The Breiddalur central volcano, eastern Iceland. *Quart. J. Geol. Soc. London* **119,** 29–63.

WALKER G. P. L. (1974) Eruptive mechanisms in Iceland. In *Geodynamics of Iceland and the North Atlantic Area,* (ed. L. KRISTJANSSON), pp. 189–201, D. Reidel Publ. Co., Dordrecht-Holland.

WALKER G. P. L. (1975) Intrusive sheet swarms and the identity of crustal layer 3 in Iceland. *J. Geol. Soc. London* **131,** 143–161.

WALKER D., SHIBATA T. and DELONG S. E. (1979) Abyssal tholeiites from the Oceanographer fracture zone. II. Phase equilibria and mixing. *Contrib. Mineral. Petrol.* **70,** 111–125.

WALSH J. B. (1965) The effect of cracks on the uniaxial elastic compression of rocks. *J. Geophys. Res.* **70,** 399–411.

WALSH J. B. (1981) Effect of pore pressure and confining pressure on fracture permeability (abstr.). *Int. J. Rock Mech. Min. Sci. Geomech.* **18,** 429–435.

WALSH J. B. and DECKER E. R. (1966) Effect of pressure and saturating fluid on the thermal conductivity of compact rock. *J. Geophysical Res.* **71,** 3053–3061.

WALSH J. B. and DECKER R. W. (1971) Surface deformation associated with volcanism. *J. Geophys. Res.* **76,** 3291–3302.

WANG H., TODD T., RICHTER D. and SIMMONS G. (1973) Elastic properties of plagioclase aggregates and seismic velocities. In *The Moon: Proc. of the Fourth Lunar Sc. Conf. 4-3,* 2663–2671.

WARD P. L. and GREGERSEN S. (1973) Comparison of earthquake locations determined with data from a network of stations and small tripartite arrays on Kilauea volcano, Hawaii. *Bull. Seism. Soc. Amer.* **63,** 679–711.

WHITEHEAD J. A., DICK H. J. B. and SCHOUTEN H. (1984) A mechanism for magmatic accretion under spreading centers. *Nature* **312,** 146–147.

WILLIAMS D. L. and FINN C. (1986) Analysis of gravity data in volcanic terrain and gravity anomalies and subvolcanic intrusions in the Cascade Range, U.S.A., and at other selected volcanoes. In *The Utility of Regional Gravity and Magnetic Anomaly Maps,* (ed. W. T. HINZE), Society of Exploration Geophysicists Publ.

YOKOYAMA I. (1985) Volcanic processes revealed by geophysical observations of the 1977–1982 activity of Usu volcano, Japan. *J. Geodynamics* **3,** 351–367.

ZUCCA J. J. and HILL D. P. (1980) Crustal structure of the southeast flank of Kilauea volcano, Hawaii from seismic refraction measurements. *Bull. Seis. Soc. Amer.* **70,** 1149–1159.

ZUCCA J. J., HILL D. P. and KOVACH R. L. (1982) Crustal structure of Mauna Loa volcano, Hawaii, from seismic refraction and gravity data. *Bull. Seis. Soc. Amer.* **72,** 1535–1550.